AUTONOMOUS UAV PRECISION ITEM PICKUP

A Thesis
Presented to
The Academic Faculty

by

John F. Papayanopoulos

In Partial Fulfillment
of the Requirements for the Degree
Masters of Science in the
Woodruff School of Mechanical Engineering

Georgia Institute of Technology
December 2017

AUTONOMOUS UAV PRECISION ITEM PICKUP

Approved by:

Dr. Jonathan Rogers, Advisor
School of Mechanical Engineering
Georgia Institute of Technology

Dr. Aldo Ferri
School of Mechanical Engineering
Georgia Institute of Technology

Dr. Kathryn Wingate
School of Mechanical Engineering
Georgia Institute of Technology

Date Approved: December 1, 2017

In loving memory of my father, Professor Lee Papayanopoulos, whose guidance was my inspiration and image is my aspiration.

ACKNOWLEDGEMENTS

I would like to thank my advisor, Professor Jonathan Rogers for his guidance and the opportunity to work on such a gratifying project. I would also like to thank my family, especially my mother, Patricia Rotonda, and my uncle, Constantine Papayanopoulos, for their continuing encouragement and support. Finally, I would like to thank NG Turf for assisting in the success of this project by allowing free use of their privately owned sod farm for testing at any time.

TABLE OF CONTENTS

LIST OF FIGURES

LIST OF SYMBOLS AND ABBREVIATIONS

θ	The roll of the aircraft
φ	The pitch of the aircraft
θ_d	The desired roll of the aircraft
φ_d	The desired pitch of the aircraft
θ_g	The roll (pan) of the camera gimbal
φ_g	The pitch (tilt) of the camera gimbal
Δx	Position of the target on the frame of the camera along the *x*-axis
Δy	Position of the target on the frame of the camera along the *y*-axis
z	Aircraft altitude
E	Max Pan/tilt error
t	Time

SUMMARY

In recent years, unmanned aerial vehicles (UAVs) have become increasingly useful in a wide range of applications such as surveying, package delivery, and recreation. An emerging research area is that of autonomous precision landing for package pickup and return to base procedures. The motivation of this project is to develop a modular UAV dock and attachment system capable of payload attachment and autonomous return to base procedures. This modular design must also support the use of multiple attachment points for cooperative package pickup.

This project develops technologies and techniques to allow a single rotary winged unmanned aerial vehicle to locate and retrieve a payload on the ground. The contributions of this thesis include an autonomous control algorithm for precision docking and a mechanical design of a docking mechanism. The control algorithm implemented uses a vision based infrared beacon-camera pair for terminal guidance feedback. Both the control algorithm and prototype docking mechanism are implemented using a quadrotor platform. Included is a detailed description of the control algorithm, mechanical design of the docking mechanism, prototype implementation, and flight test results. The results of this work show the suggested methods are reliable and may be useful in a variety of applications in which UAVs retrieve supplies or personnel for subsequent transport.

CHAPTER 1. INTRODUCTION

In recent years, unmanned aerial vehicles (UAVs) have become increasingly useful in a wide range of applications including, but not limited to, construction and infrastructure surveying, military reconnaissance and logistics, package delivery, and recreation. The versatility of UAVs allows for the completion of many tasks that include payload transportation or observation. With the increasing use of autonomous UAVs (aUAVs) for these purposes, there is a growing need for docking and attachment mechanisms that can function without the presence or assistance of a human.

A problem space that has been the focus of attention is that of autonomous aircraft payload retrieval, transport, and return to base procedures. However, little prior work has investigated the physical mechanisms required to dock with a payload or ground station robustly. With respect to vertical lift vehicles, this research explores this problem space with solutions to two primary issues: the control algorithm for the device to autonomously approach the docking position and the mechanism for localization and attachment once in contact with the dock.

1.1 System Overview

The system studied here achieves the desired task of autonomous attachment to packages or docks via an infrared camera-beacon pair for terminal guidance feedback. Terminal guidance feedback is the sensory input from the desired docking location to the sensors onboard the aircraft for updating the control law. As the aircraft approaches the target, a terminal guidance law takes control of the aircraft with the use of the camera-

beacon pair. A gimbal ensures that the camera continues to point towards the beacon such that the beacon is continuously at the center of the camera field-of-view (FOV). The angles used to command the camera to point at the beacon are used to command the roll and pitch of the aircraft, forcing it above the target location. When the aircraft is above the beacon, it descends to the target location. Once it makes contact, a passive localization mechanism positions the aircraft precisely in the center of the attachment mechanism. Once positioned correctly, the aircraft anchors itself to the attachment point using an actuator.

The method used for control consists of a PID control law that keeps the camera (which is mounted to a gimbal) positioned such that the beacon is centered in the camera FOV. The angles of the camera pan and tilt are input into another PID loop that controls the roll and pitch of the aircraft such that it is positioned above the beacon. When the error is acceptably low, the aircraft begins to descend towards the beacon. This method has several advantages, primarily that the camera is far less likely to lose sight of the beacon if the aircraft incurs lateral positioning errors as a result of external environmental disturbances.

The landing gear of the aircraft serve a dual purpose by acting as both traditional landing gear when the aircraft sits on the ground as well as providing a mechanical means of centering into the dock (attachment mechanism receptacle). When docking, the landing gear fold in such a way that the tips of the four legs touch to form an insertive cone. The attachment device (receptacle) on the payload is a ring parallel to the ground. As the aircraft descends, the point fits into the ring and positions the aircraft concentrically. Once centered, the legs finally fold out again thereby anchoring the aircraft to the dock.

In this project, a series of flight experiments were conducted in which a test aircraft was manually flown to a position with the beacon in sight of the camera (a condition which could be met through autonomous GPS based flight). Indoor and outdoor flight tests confirmed the ability of the aircraft to reliably dock in realistic flight conditions. Data was collected by storing flight data to a memory card for post processing.

1.2 Prior Work

As stated above, the subject of transportation and logistics via UAVs is a highly active research area. This section discusses some prior work in this field of research. While these topics are related, to the authors' knowledge there is very little prior work on UAV docking devices in the robotics community and thus this area is a very open research topic.

Jeffrey, Yanev, Biaz, & Murray (2014) addresses a similar solution encompassing both machine vision and optical flow methods for precision landing. In their research, the aircraft is required to land on both static and dynamic target locations. To do this, they used a modified version of the Pixhawk system with a Px4Flow optical flow sensor made by Pixhawk. The solution developed was to use a ground station for computing and transmitting waypoints that the aircraft follows on the way to the target location. When landing, the aircraft is commanded to attain a certain altitude before beginning the precision positioning. Through GPS, the aircraft attempts to get as close to the target location as possible, where it then uses the optical flow sensor for control. This sensor detects motion and can identify the pattern of the target location. By using the flow sensor, the aircraft can remain very steady in mid-air and have very high accuracy of determining its true position. This is very similar to the standard Pixhawk system, but the research done by this group

attains higher accuracy over this pre-existing method through the use of this improved algorithm and hardware. (Jeffrey, Yanev, Biaz, & Murray, 2014) In this report, it is even stated that "The most popular approach… is by far the vision based landing approach". Al-Sharman (Al-Sharman, 2015) did something similar by developing his own autonomous take-off and precision landing system using GPS, inertial measurement, and optical flow. The author used state-estimation to further enhance the accuracy of these systems for precision control.

While most systems use optical methods for controlling aircraft in terminal flight, there is no precedent in the literature (to the authors' knowledge) for using active beacon tracking for terminal guidance, as is used in this project.

Many inventors have attempted to develop methods for autonomous UAV docking, as evidenced by several patents that exist in this area. These provide good background to this problem space, but few detailed solutions have been proposed. Most similar to one of the methods considered in this project, but not used, was that of a patent entitled "Intelligent self-leveling docking system" by Godzdanker, Valavanis, and Rutherford (United States of America Patent No. 2014/0124621 A1, 2010). This patent discloses a method where the aircraft lands on a platform. It is subsequently pushed by mechanical sweepers into the center of its platform where it can be automatically latched and refueled.

A concept described by Gentry, Hsieh, and Nguyen provides some additional docking mechanisms for UAVs (United States of America Patent No. 9,387,928 B1, 2014). It also suggests the use of a network of "multi-use UAV" where aircraft can be versatile in uses for a community. This work is relevant because it suggests the use of docking with

respect to multi-UAV systems, but these docks are intended, again, as home locations for the aircraft to perform common tasks of renewing energy reserves or package drop-off and pickup. All shown methods include a platform for the aircraft to land on with various mechanisms for holding the aircraft in place. Examples provided are latches that hold the landing gear down, sleeves for the landing gear to fly into, small housings for the aircraft to land inside of, and electromagnets for holding the aircraft in place. The examples provided for package pickup show the package being handed off to the aircraft at this dock location. This system may work well in autonomous package delivery, but does not provide solutions to package pickup of variable package sizes and locations. These solutions are also not inherently robust to positioning errors during docking.

Other inventors suggest solutions only to the problem of passive precision positioning and attachment. Prakash and Ceribelli (United States of America Patent No. 2016/0196756 A1, 2014) suggest the use of a landing platform with grooves for the landing gear to land in followed by the actuation of "guide arms" which swing on top of the landing gear, trapping the aircraft in place. Wang (United States of America Patent No. 9,346,560 B2, 2014) suggests the use of landing legs with convex cones at the tips of each leg to land in receptive concave cones to localize the aircraft for recharging tasks. These mechanisms, while having similar motivation to the current work, are quite complicated compared to the design proposed here.

Marshall (United States of America Patent No. 7,398,946 B1, 2004) suggests the use of a hook on an aircraft for aircraft retrieval. This mechanism would hook onto hanging lines for attachment. A related project developed by Lovell, Hui, and Umbreit (United States of America Patent No. 2009/0294584 A1, 2008) suggests the use of a robotic arm to

attach to the aircraft in midair. The aircraft equipped with a hook will fly past this attachment point and be captured. This concept is interesting because in the discussion provided, it suggests this mechanism be attached to a ship where the robotic arm is meant to stabilize the attachment point. This suggests this method is highly mobile where the aircraft can attach to a moving base location.

Beardsley *et al*. (United States of America Patent No. 2016/0039541 A1, 2014) seem to particularly acknowledge the issue of precise positioning of the aircraft during the landing procedure with a complex design for a docking mechanism. Control algorithms can be tuned to be precise, but the issue of precise positioning may persist as these control algorithms may not achieve precise enough tracking for reliable attachment. Ref. (United States of America Patent No. 2016/0039541 A1, 2014) is the only patent that seems to seriously take into consideration the issue of precise positioning such that the attachment would be robust. The system presented in this work uses an infrared camera at the base station directed upwards with infrared LEDs on the aircraft. This is used for terminal feedback. The dock has sloped surfaces "arranged in a crown pattern" which the landing gear slides along as it is directed into grooves for the aircraft to come to rest in. This mechanism is somewhat similar to that proposed here, but requires a more substantial and cumbersome receptacle device on the payload compared to that considered here.

1.3 Thesis Organization

This thesis will cover the topics described above by first discussing the mechanical design of the dock and control synthesis of the terminal guidance algorithm. Chapter 2 details the concepts considered and used for the attachment mechanism. Chapter 3 details

the control algorithm that was developed for this project. Chapter 4 provides a detailed description of the prototype flight system and hardware experiments. Finally, Chapter 5 describes the results achieved and recommendations for future work.

CHAPTER 2. ATTACHMENT MECHANISM

During a landing procedure, there is an inherent position error that will come from various sources including environmental conditions, inaccuracy and noise of sensors, control system delays, and other non-ideal variability in real world applications. Within the scope of this project, a position error in landing of the control algorithm is expected. Therefore, it is imperative to have a system mitigating this error by precisely positioning the aircraft beyond what the control algorithm can do. This precise positioning is necessary for the physical attachment to be reliable and not jam, slip, or miss altogether. Additionally, for the future application of multi-quadcopter cooperative lifting, it is important for all vehicles to be securely attached to the payload prior to flight.

In addition to this precise positioning, the aircraft must be able to rigidly attach itself to the payload reliably. Once in position, there are various methods that can be conceived for this attachment, but, for this project, a mechanical actuation method is used.

This chapter will detail the single system concept devised for achieving both the precise positioning and rigid attachment tasks.

2.1 Positioning Methods

The concept of precise positioning, in the context of this project, is a way of mechanically positioning the aircraft through contact with the docking location. Below are some concepts that were considered in the course of this work, and the reason(s) why they were not selected for use.

2.1.1 Plumb Line

The first design concept was to have the aircraft lower a line during flight. As the line sways over the target area, it would be attracted via magnetic forces or, if precise enough, simply hook onto the target. Once attached, the line would be reeled in, thereby pulling the aircraft into position. An advantage of this design is that it allows for the aircraft to delay landing until there is full certainty of a successful landing procedure. Another advantage is its used of a physical guide mechanism rather than total reliance on a sensor for terminal feedback guidance.

The limitations of this design come from its dependence on precision. The precise altitude must be known for this method to succeed, which may be difficult to obtain using lightweight or low-cost sensors. The aircraft must then maintain constant altitude throughout the terminal locating process such that the height of the end of the line relative to the terminal location is constant.

Additionally, this method assumes that the plumb line will happen to sway precisely over the targeted area. This requires the aircraft to hover for an undetermined amount of time before making contact. Windy conditions may present significant problems as the line may be blown in unpredictable directions. Thus, this method requires a somewhat complicated system on the aircraft and on the ground, and was not selected for further investigation.

2.1.2 Dock Sweepers

The second precise positioning method considered was to have mechanical devices position the aircraft once it has landed. Specifically, this system would allow the aircraft to first land on the targeted landing area as precisely as can be done using only a control algorithm and sensors. Once landed, a system of sweepers would extend, pushing the aircraft precisely where it needs to be. As mentioned in Ref. (United States of America Patent No. 2014/0124621 A1, 2010), this is a method that has been conceived by others for precise positioning purposes.

An advantage of this system is that there is no hardware required on the aircraft for positioning. This lack of onboard hardware means that the aircraft would be lighter, leading to longer flight times and better agility. The primary disadvantage lies in the complexity of the positioning system. This may be acceptable in applications where the dock is a home location, but is unacceptable for the purposes of package pickup, as the dock may be quite heavy, complicated, and/or expensive. This system would require a mechanical device to be attached to a payload that has a large area for the aircraft to land on. Such a cumbersome system would likely be heavy and produce payload drag which the aircraft would have to overcome for package transport missions. Thus, this method was not considered further for the purposes of this project.

2.1.3 Ring with Clips

The third method considered was to use a ring that the aircraft would descend onto. The landing gear of the aircraft would be angled apart such that they would form a wireframe cone that is receptive to the ring. The area of the ring would be the same as the area on the bottom of the aircraft between the landing gear. Clips attached to the landing

gear would prevent the payload from slipping off after the aircraft has landed. The primary advantage to this system is that it is fully passive, requiring only structural components. It can be considered a disposable component that can be easily attached to a payload and landed upon. The primary disadvantage is that it is possible in certain orientations for the legs to miss the ring during landing, as shown in Figure 1. This is primarily due to the legs being used as a wireframe receptive component. This requires the ring to be an insertive portion and therefore relatively small. This issue can be mitigated by the introduction of more material between the legs, but if more material is added there will be additional weight and drag on the system.

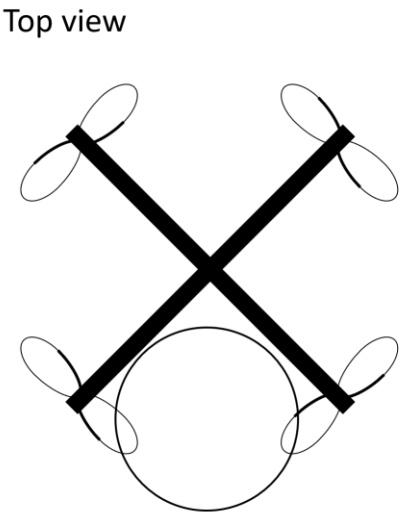

Figure 1: Failure case of unused design.

A rudimentary prototype of this concept was created for testing. To implement this method, a wireframe cube was used. A cube was used because it is effectively a square ring offset from ground by the height of the aircraft when it is landed. A square ring was preferred here because the platform used has four legs. Having one leg on each side of the ring also forces the aircraft to attach at a specific yaw angle relative to the payload.

However, the lack of robustness of this system, and the need to create a specialized wireframe, led to rejection of this design concept for this project.

2.2 Basic Concept for Selected Positioning Method

The basic concept selected for vehicle docking for this project is the use of an *insertive* cone and *receptive* ring combination where the vehicle landing gear is the insertive and the attachment point is the receptive component, respectively. This is unlike the method described in section 2.1.3 where the vehicle was receptive and the dock insertive. Typically, this geometry would not be reliable in a passive system as compared to an insertive and receptive dual-cone system. This is because there would be nothing to force the axes of the ring and cone to remain parallel which would lead to the cone rolling over such that it is no longer upright. This is not an issue in this case as the vehicle is not passive and through its own control algorithm tends to keep itself upright.

2.3 Concept for Attachment Mechanism

An intuitive system for attachment typically consists of some actuated components. Frequently this may be a gripper or latch system. The concept used in this project was an actuated anchor system. The attachment arms are lowered through the ring during landing, and are then spread out into the ring such that they may not slip back out.

2.4 Combining Concepts

In the case of flying aircraft, the less material that is needed onboard for tasks to be completed the better since weights savings leads to increased payload capacity. In this design, the above two concepts (as well as aircraft landing gear) were combined into one

simple system. In this way the increased weight of the base aircraft was minimal with respect to the total lifting capacity.

2.4.1 Physical Design

This system assumes that the vehicle being used has landing gear for a quadcopter that consists of arbitrary *n* straight legs that are angled apart such that the base of the landing gear is wider than the area covered by the aircraft-landing gear attachment points. These legs must then be hinged so that they may rotate together to a point or away from each other. The legs are then actuated such that the angle of the legs may be controlled. For the rest of this discussion, the positions of the landing gear shown in Figure 2 shall be referred to as Positions 1 and 2.

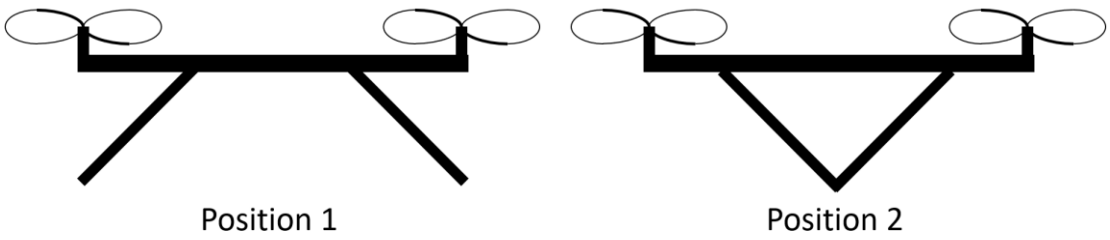

Figure 2: Landing gear position name scheme.

Using these angle-controlled legs allows for standard landing and, when coupled with a landing ring, for precise passive positioning and attachment. Position 1 is the standard position of the quadcopter legs and can be used for typical landing. It can also be used when inserted into the dock to anchor the vehicle to the attachment ring. When in Position 2, the landing gear fold such that the tips of the four legs touch to form a cone. The ring is parallel to the ground offset by at least the length of the legs. As the aircraft

descends, the ring is used to receive the cone formed by the legs in Position 2. The point of the cone fits into the ring and positions the aircraft concentrically. The legs finally fold out again to Position 1 and can no longer slide out of the hoop. The aircraft is thus rigidly attached to the dock in all degrees of freedom except yaw. In this implementation, rotation about the yaw axis with respect to the payload does not occur as there is significant friction between the attachment mechanism and the docking ring. This ring could also have different shapes or grooves as to rigidly attach the device to the ring. The scheduling of these positions during flight is discussed below.

2.4.2 System Order of Operation

Whether the aircraft is starting from docked or sitting on the ground, the aircraft will always start from Position 1 (with small variation in scheduling of events for take-off/landing procedure). Assuming the aircraft begins on the ground, it will takeoff from Position 1 and during flight will change to Position 2. Position 2 will likely give the aircraft less rotational inertia so, depending on preference, when this transition occurs may be different depending on circumstances of use. In either case the aircraft must be in Position 2 during the docking procedure. The aircraft will land inside of the ring using a control algorithm. Once in place, it will change back to Position 1, thereby locking it in place. This is illustrated in Figure 3.

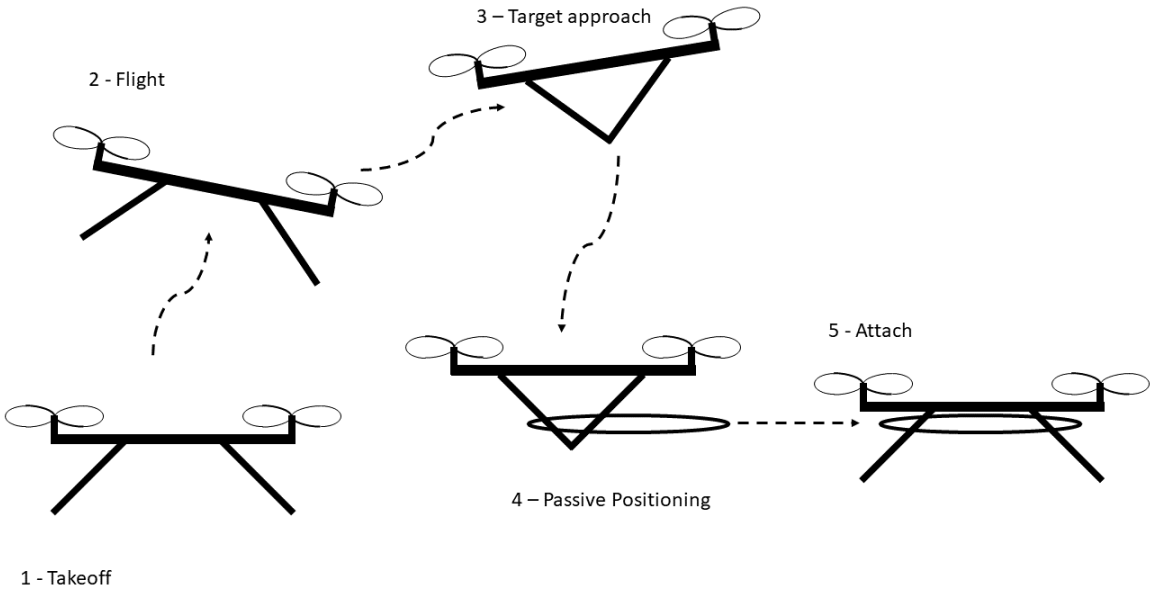

Figure 3: Full flight procedures.

If the aircraft begins from inside the dock, this procedure varies only slightly. Before takeoff, the legs must first transition to Position 2. Once it is airborne enough such that the legs are completely outside of the dock, the procedure remains the same as if it had taken off from the ground.

2.4.3 Advantages Over Other Systems

The positioning and attachment mechanism developed for this project has unique advantages over other docking concepts, allowing it to achieve all required tasks with minimum overhead. The three main advantages are that the concept is light, mechanically simple and reliable. The light weight and low drag profile of this design means that an aircraft can be equipped with this dock and fly with the payload with minimal resistance due to the attachment mechanism itself. The dock requires a single actuation of all legs together to achieve both tasks of precise positioning and attachment. Finally, as long as the

point of the legs in Position 2 is within the ring during landing, the device will precisely position itself into the center of the ring passively, and come to rest in a position where it is ready to attach. There are no obvious cases where this system may fail unless the point at the center of the legs is lowered outside of the ring.

2.4.4 Limitations

The most important limitation to mention is that the docking ring on the payload must be offset from the ground a distance of at least the length of the legs being used. This is so that the legs are able to transition from Position 1 to Position 2 while inserted into the dock, and vice versa. There must be an unobstructed path for the legs to swing such that they will not come in contact with the ground or any other structure.

CHAPTER 3. CONTROL ALGORITHM

In order to achieve the localization methods and attachment described previously, the aircraft must first be able to approach the localization point. This project focuses only on the landing procedure. It is assumed that either through automated or manual flight the aircraft can already position itself within sufficient proximity to the dock/beacon such that the beacon at the attachment point is within the view of a camera onboard the aircraft. Once in sight of the camera, the precision landing algorithm can take over. This is a concept that has already been implemented, most predominantly by Pixhawk with their precision landing algorithm. This existing implementation was found to lack sufficient tracking accuracy, and a new control scheme was developed for this project.

All methods described in this section include a camera/target system. The target is situated on the ground at the dock (attachment point). The camera is mounted to the aircraft and is attached via a two-axis gimbal capable of rolling and pitching the camera with respect to the aircraft.

3.1 Methods Explored

A number of ways for controlling the device were explored including using an implementation where the camera is statically attached. Also explored was the idea of using a motion-compensation method where the camera is gimbaled such that it always is level with the ground. In this way, the roll/pitch of the aircraft does not affect the orientation of the camera in the inertial frame (which is always pointed straight down).

3.1.1 Statically Mounted Method

This is the method used in the Pixhawk system (Precision Landing and Loiter with IR-LOCK, 2017). Here the camera is statically mounted to the aircraft and the target is acquired by using the *x-y* position of the beacon in the frame of the camera (*Δx* and *Δy)*. In the Pixhawk implementation, this position error in the camera frame is used with a simplifying assumption of the target being a constant 1m from the aircraft and a unit vector is generated pointing at the target. This error vector is passed on to the autonomous control algorithm of the Pixhawk system.

In the attempted implementation done by this project, the *x-y* position error in the camera frame was passed to a PID loop that outputs desired roll and pitch to correct these errors. While it is possible to feed this position error to a velocity PID controller, there is currently no way to measure the vehicle's velocity on the prototype aircraft and determining velocity from the camera sensor would have led to unacceptable inaccuracies. Regardless, this method was shown to work in theory, but as it suffers from the same implementation issues as the Pixhawk system (ie. the true position is affected by the roll/pitch of the aircraft and that it is easy to lose the target close to the ground), it was deemed insufficient.

3.1.2 Pseudo-Static Mounted

To mitigate the coupling effect of target position on the camera frame being affected by the roll/pitch of the aircraft, a pseudo-static system was considered. This means the camera was mounted to a 2D gimbal where the roll and pitch of the aircraft was negated by the gimbal such that the frame of the camera would remain parallel with the ground. The same tracking control algorithm as that described above was attempted using this

system. While the issue of roll/pitch affecting the beacon location measurements in the camera frame was resolved, the issue of the camera losing the beacon when close to the ground was still an issue. Additionally, as the gimbal cannot achieve a correct orientation instantaneously, some additional lag was introduced to the system.

3.1.3 Gimbal Tracking Mounting

The selected method for obtaining beacon measurements for tracking was to have the camera gimbal system follow the target. Using the *x-y* position of the beacon on the frame of the camera, a PID loop is used for controlling the gimbal such that the target is always centered in the frame of the camera. For this discussion, the roll and pitch of the camera will be referred to as the pan and tilt, respectively. The pan/tilt of the camera required to point the camera at the beacon are used for commanding the roll/pitch of the aircraft to drive it towards the beacon. The zero-error state is when the gimbal is pointing the camera directly downwards in the frame of the quadcopter. This method has several advantages. The most valuable advantage is that once the camera first locks onto the target, it is less likely that the camera will lose sight of the beacon as the vehicle manoeuvres during descent.

3.2 Control Method

The control method used in this project fundamentally relies on the camera control process described in section 3.1.3. The camera is mounted to the device using a 2D gimbal where it is commanded to a desired pan and tilt. This pan and tilt are computed using a PID loop to force the target to the center of the camera frame. Another PID loop is then used where the input is the camera pan/tilt and the output is a desired roll and pitch angle of the

aircraft. The desired roll and pitch angles are then tracked by the vehicle autopilot's PID stabilization loop. A block diagram of this process is shown in Figure 4.

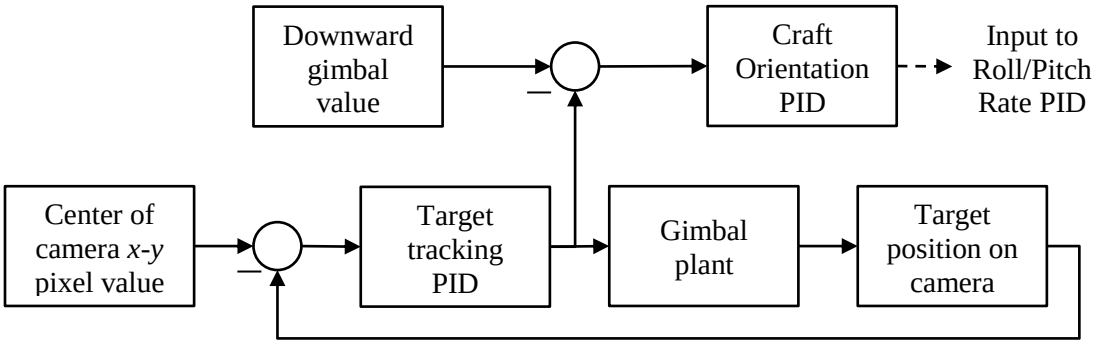

Figure 4: Control algorithm block diagram.

Not shown in Figure 4 is the effect of the desired aircraft orientation on the target position in the frame of the camera. The desired aircraft orientation is coupled with the relative position of the target location. Therefore, there is an effect of the aircraft orientation PID on the target tracking PID. However, as the rotation of the aircraft is relatively slow compared to the angular velocities of the gimbal, there is sufficient time scale separation such that this interaction can be ignored.

3.2.1 General Aircraft Controls

The stabilization loops used in most multirotor aircraft are fairly standard. There are four typical input commands: roll, pitch, and yaw rates and thrust. In a fully manual system, the user must command each of these directly with little alteration of signal from the user to the controls of the aircraft. Typically, this is insufficient for even the most experienced users. In a "manual" control mode there is usually a PID loop used for a user to command a desired roll/pitch/yaw rate where an IMU is used to determine measured angular rates and an appropriate value is output to the motors. In an auto-levelling system,

desired roll/pitch/yaw angles are provided and a PID loop is used to determine desired control inputs. For thrust control, another PID loop is used where the desired altitude is provided to the loop as a setpoint and a barometer (and occasionally a rangefinder) are used to measure the actual altitude. In the implementation used in this project, this PID loop provides desired vertical velocity. The result is then used in another PID loop that controls desired thrust.

The pre-existing auto-levelling and auto-altitude control loops from the UAV manufacturer (Parallax) used in this project were used as a starting point and modified for the project as needed. In this implementation, without any input from the control algorithm developed as part of this work, the aircraft would attempt to keep itself level and at the same altitude. Using the controls described later in this chapter, this system can be augmented with additional outer control loops and autonomous flight towards the dock is achievable.

3.2.2 Camera Control Loop

As stated earlier, the camera is mounted to a 2D gimbal. When the target is viewable in the frame of the camera, the *x*-*y* position (Δx and Δy) of the target in the camera frame is computed. This value is processed by two independent PID loops as the measured error where the setpoint is the center of the camera frame. The output of these loops is a desired angle for the pan and tilt motors respectively (θ_g and φ_g). These angles, in addition to commanding the angles of the gimbal motors, are passed on to another set of PID loops for commanding roll and pitch of the aircraft.

3.2.3 Desired Orientation Loop

Using the PID outputs to the camera gimbal as described in section 3.2.2, the aircraft may be controlled. The logic here is that the angles necessary to point the camera towards the beacon provide information as to how the aircraft must be commanded such that it moves towards the beacon. If the aircraft is not directly over the beacon, there is an error that can be corrected until the aircraft and the indicated direction are aligned. In this case, the desired alignment is for the camera to be pointing straight down.

The angle of the camera is passed on to a PID loop as the measured value where the setpoint is the camera pointing straight down (relative to the aircraft). The output is a desired angle the aircraft should have such that it propels itself in the direction of the target. This process is shown below in Figure 5.

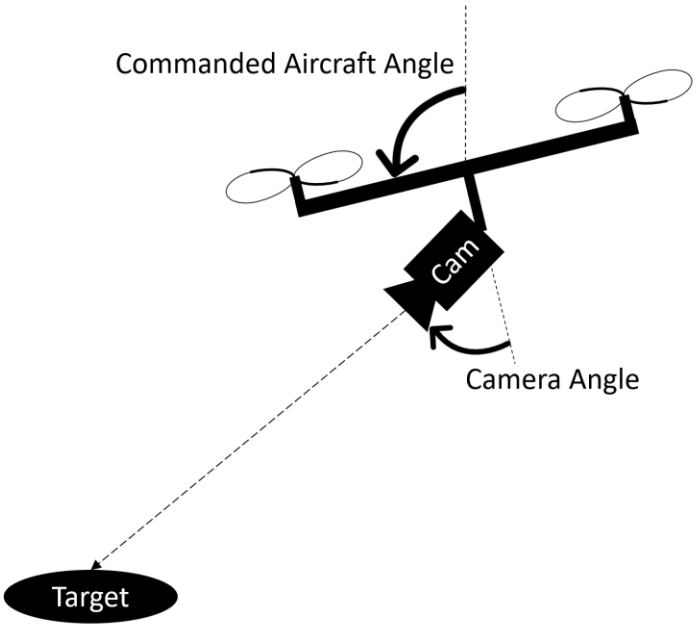

Figure 5: Camera angle to aircraft angle.

As can be seen in the figure, to do this the vehicle must turn itself in the opposite direction of the camera which thereby increases the error in the angle of the camera. The

PID loop controlling the angle of the aircraft is limited so that the commanded pitch and roll angles do not grow beyond an acceptable range.

The definition of a PID controller is shown below in Equation 1

$$u = K_p e + K_i \int_0^t e\, dt + K_d \frac{d}{dt} e \tag{1}$$

where u is the PID controller output, K_p, K_i, and K_d are the proportional, integral, and derivative gains, respectively, and e is the error between the setpoint and the measured. All PID loops described here use a discretized version as shown below in Equation 2

$$u_k = K_p e_k + K_i \sum_{n=0}^{k} e_k + K_d (e_k - e_{k-1}) \tag{2}$$

where k is the indicator of the time step in the iterations of the program loop. As time is reasonably constant between iterations of the loop, time can be compensated for in the integral and derivative gains. If the angle of the camera pointing straight down with respect to the aircraft is 0 deg, then the equations for controlling the orientation of the aircraft would be as follows in Equations 3 and 4

$$\theta_{d_k} = -(K_p\theta_{g_k} + K_i\sum_{n=0}^{k}\theta_{g_k} + K_d(\theta_{g_k} - \theta_{g_{k-1}})) \quad (3)$$

$$\varphi_{d_k} = -(K_p\varphi_{g_k} + K_i\sum_{n=0}^{k}\varphi_{g_k} + K_d(\varphi_{g_k} - \varphi_{g_{k-1}})) \quad (4)$$

where desired roll and pitch θ_d and φ_d at time step k is the inverse of the PID controller provided in Equation 2. The error value is the gimbal pan, θ_g, in Equation 3 and gimbal tilt, φ_g, in Equation 4. As illustrated above in Figure 5, the inverse is used as it is desired for the aircraft to pitch and roll in the opposite direction of the gimbal so that the aircraft flies towards the target location.

3.3 Landing Procedure

The fundamental objective of the controls described above are to position the aircraft directly above the target. In order to dock properly, the aircraft must descend towards the target while remaining centered above the beacon.

There are many ways of achieving a landing procedure. In this implementation, the thrust controller is driven by a desired altitude. The rate of descent could be constant, where each iteration of the control loop the desired altitude is changed by a constant *dz*. This is perfectly acceptable if the only goal is to land and not to consider a precise landing location. With a controller that keeps the aircraft exactly over the beacon, a constant descent rate would also work, but this is somewhat impractical as the aircraft is likely to drift due to winds for instance. A more reasonable solution is to use a dynamic descent rate. This may be a binary descent rate where it either descends at a constant rate if within an acceptable

range or hover when the error is large. Alternatively, it can be a linear or higher order descent rate calculation where, depending on the amount of error, the aircraft may descend at a varying rate. In this project, the latter method was adopted where a linear descent scheme was utilized.

The total position error for determining descent rate is based on the pan and tilt error. How this total position error is computed could occur in multiple ways. For this project, the max absolute value of the two errors was used (L^{∞}-norm). As the pan and tilt errors can be considered to be relatively independent, this scheme will descend at an acceptable rate for the control loop with the greater error.

The effect of this descent algorithm will be referred to as a cone of certainty. A cross-sectional visualization of this is shown below in Figure 6. The tip of the cone represents the location of the target. The aircraft will attempt to position itself along the center axis of the cone. When the aircraft is inside this cone, it's downward velocity will correspond to the color code where green is maximum downward velocity and red is no descent rate. Anywhere outside this cone will also have a zero descent rate.

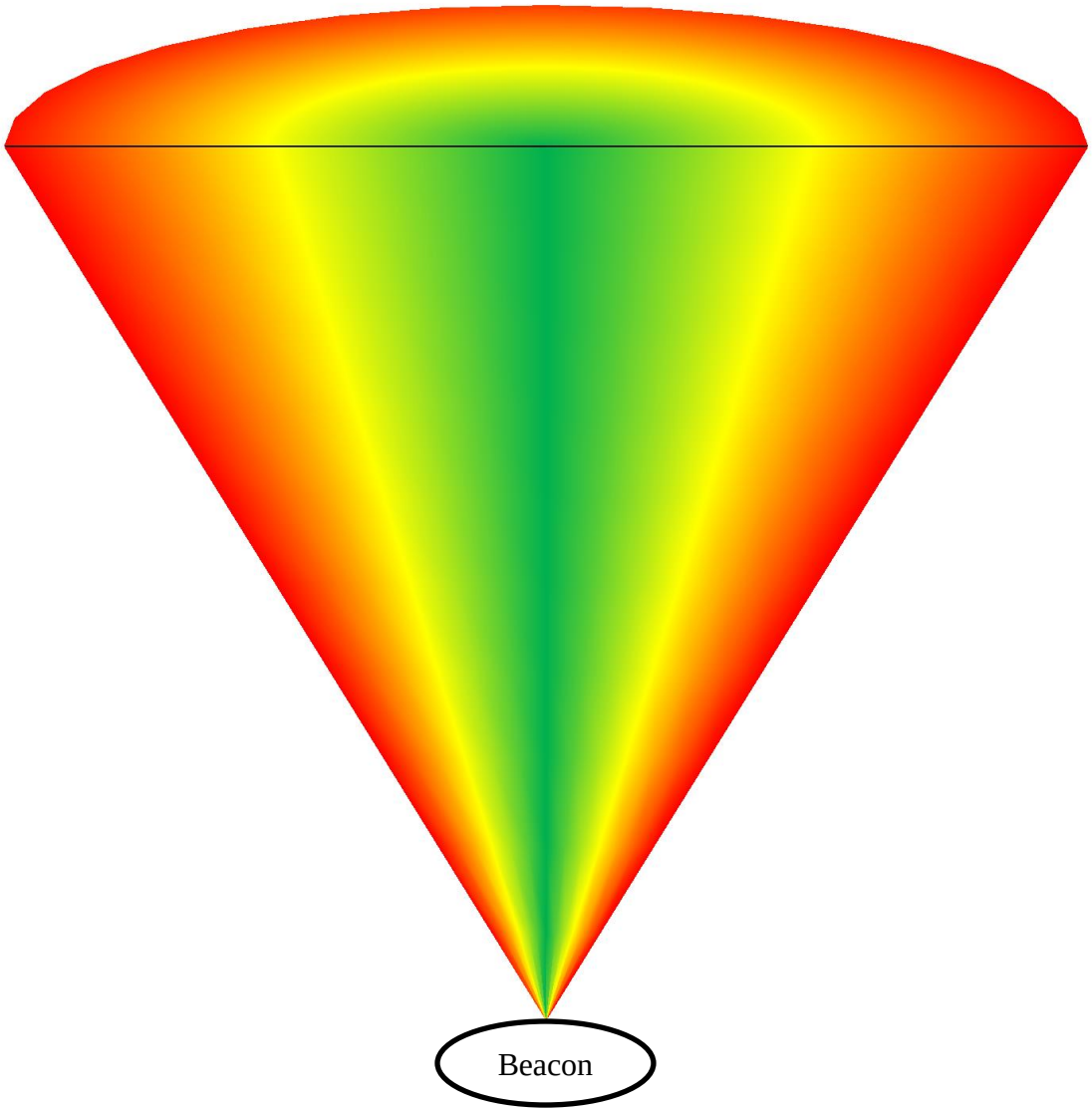

Figure 6: Cone of certainty.

The descent rate is computed using a linear relationship expressed in Equation 5

$$dz = (-aE + b) * dt \tag{5}$$

where error *E* is calculated using Equation 6, *b* is the maximum desired descent rate, *b/a* is the maximum permissible angle error and *dt* is the time between iterations.

$$E = \max(|\theta_g|, |\varphi_g|) \tag{6}$$

The sign convention used is that altitude is measured from ground level meaning that altitude increases moving upwards away from ground. At low errors, *dz* equates to a positive value and is therefore subtracted from the desired aircraft altitude. As the error *E* increases, *dz* approaches 0. This function is saturated such that *dz* cannot become negative as this would cause the aircraft to climb.

CHAPTER 4. EXPERIMENTAL SYSTEM

This chapter aims to describe the hardware and mechanical components to implement the methods detailed in the previous chapters. Included are names of prefabricated products, CADs and photographs of items prototyped for this project, and codes used for controlling the device.

4.1 Prefabricated Components

Many components used in this project were prefabricated electronics that are either standalone or parts of kits. This section outlines all prefabricated components used throughout the course of this project.

4.1.1 Elev-8 v3 Experimental Quadcopter Platform

The platform used for this project is the Parallax Elev-8 v3 quadcopter kit. This kit contains the motors, frame, and microcontroller with necessary sensors for basic flight (IMU and barometer). The image of this product from the Parallax store page is shown in Figure 7. The microcontroller used was the Rev-B version and uses the same Propeller chip found on other Parallax microcontrollers. The firmware for flight is available from Parallax. It is fully open source and can be opened directly in the Parallax IDE. This code was used as the starting point as it is intended to be the code necessary for a user to have assisted flight (auto-levelling and hover capabilities). This code contains no autonomous flight features so these features were added into the code for the purposes of this project.

Figure 7: Original Elev-8 platform. (ELEV-8 v3 Quadcopter Kit, 2017)

Other components used with this kit for basic flight include a battery pack, radio transmitter and receiver for manual control, and a pair of transceivers for telemetry. The batteries used with this kit are 3300 and 5300 mAh 3 cell lipos. The radio used to manually control this device is a 2.4GHz controller using DSMX protocol to communicate with a JR satellite receiver. This receiver communicates with the Parallax microcontroller over a

single serial DSM line. The telemetry radios are a pair of XBee 900MHz modules; one on the aircraft, one at a base station computer.

4.1.2 Servo Components

Onboard this aircraft are three servo motors: one for actuating the legs and two for gimbal control of the camera. The servo for actuating the legs is an Align brand DS610 standard size digital servo. The other two servos are TowerPro brand SG92R digital micro servos. These two micro servos are each used for one axis of the camera gimbal.

4.1.3 Pixy Camera-Beacon Pair

As stated earlier, the sensor used for terminal guidance feedback control is a camera-beacon pair. This is a kit made by IR-Lock and consists of an infrared beacon and camera. The beacon is an array of infrared LEDs on a PCB. The camera is a CMUcam5 (Pixy camera) made by the CMU team of Charmed Labs and Carnegie Mellon. It is a machine vision platform that can be trained to identify objects through machine vision onboard the camera's microcontroller. This is then output as a Δx and Δy position in the frame of the camera. For this kit, the camera also has a filter on the lens that only allows the frequency of the beacon to pass through.

4.1.4 Arduino Microcontroller

The Pixy camera was designed specifically for communication with an Arduino. There are porting guides for the camera to communicate with other platforms. These ports are not always perfect and when this was attempted with the Parallax Propeller board, there were issues with missed messages. With more troubleshooting, this likely can be corrected,

but it was not considered important in the scope of this project. An Arduino Nano microcontroller was inserted in-line between the camera and the Parallax microcontroller to decode the position of the beacon via SPI communication protocol, run the camera gimbal controls and transmit the gimbal angles via UART to the Parallax microcontroller.

4.1.5 Naze32 Flight Controller, JR PMW Receiver and Pololu Multiplexer

For safety reasons, an additional flight controller and receiver were used to enable emergency takeovers. The multiplexer is meant to transfer control of the motors from one processor to the other.

4.2 Custom Components

Custom components were necessary for the attachment mechanism and gimbal to control the camera. Below is a description of these components.

4.2.1 Localization and Attachment Mechanism

The concept described previously in section 2.4 was implemented to allow for positioning and attachment of the aircraft for the purposes of this project. This requires actuated legs and a ring for the legs to settle and lock into. The legs of the original Parallax Elev-8 platform were replaced with aluminium L-extrusions and a hinge. The hinge in this implementation is 3D printed using fused deposition modelling (FDM) and allows each leg to rotate 90 degrees.

The current design uses legs that are the correct length to allow for 45 deg rotation of the legs in both Positions 1 and 2. This was done as it is an optimum of two equally

weighted objectives. One objective is to maximize the slope of the insertive cone. The greater this slope is, the less sliding friction there is and the more likely the aircraft will not stop descending into the ring until fully in position and the more gradual the positioning task is. The other objective requires a minimization of the slope of the insertive cone. The shorter the cone is, the less the tip will move with the rotation of the aircraft as the control algorithm attempts to position the aircraft above the ring. If the cone is very long, a small input command to roll or pitch the aircraft will mean a larger rotation of the tip of the cone which could lead to unsuccessful docking. Therefore, a 45 deg angle of each leg was used to balance these two objectives.

Shown in Figure 8 and Figure 9 are textured CADs of the attachment mechanism to illustrate the position of these components on the Elev-8 platform. Figure 8 has been numbered to help explain each component. Item 1 is a single boom of the Elev-8 quadcopter. Item 2 is a single leg of the landing gear. Item 3 is the hinge in which the leg is fitted and can rotate 90 deg. Item 4 is a pushrod which is connected to the standard servo motor and is what actuates the landing gear. Figure 8 shows the landing gear in Position 1 (as described earlier) and Figure 9 shows the landing gear in Position 2.

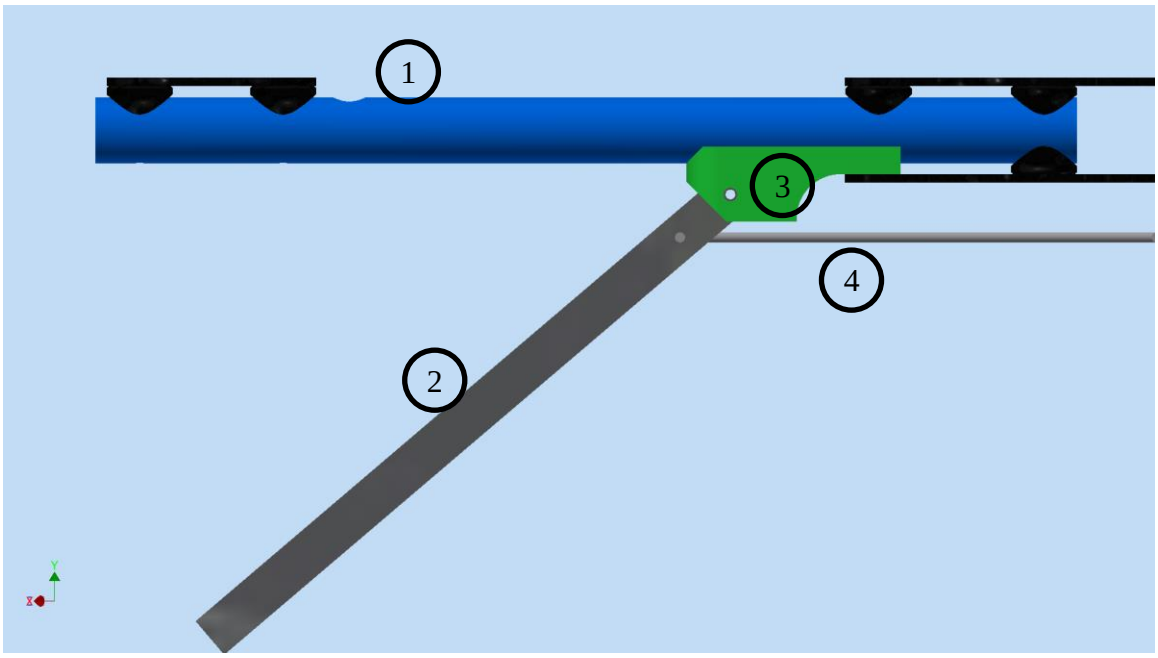

Figure 8: Side view of single landing gear – Position 1.

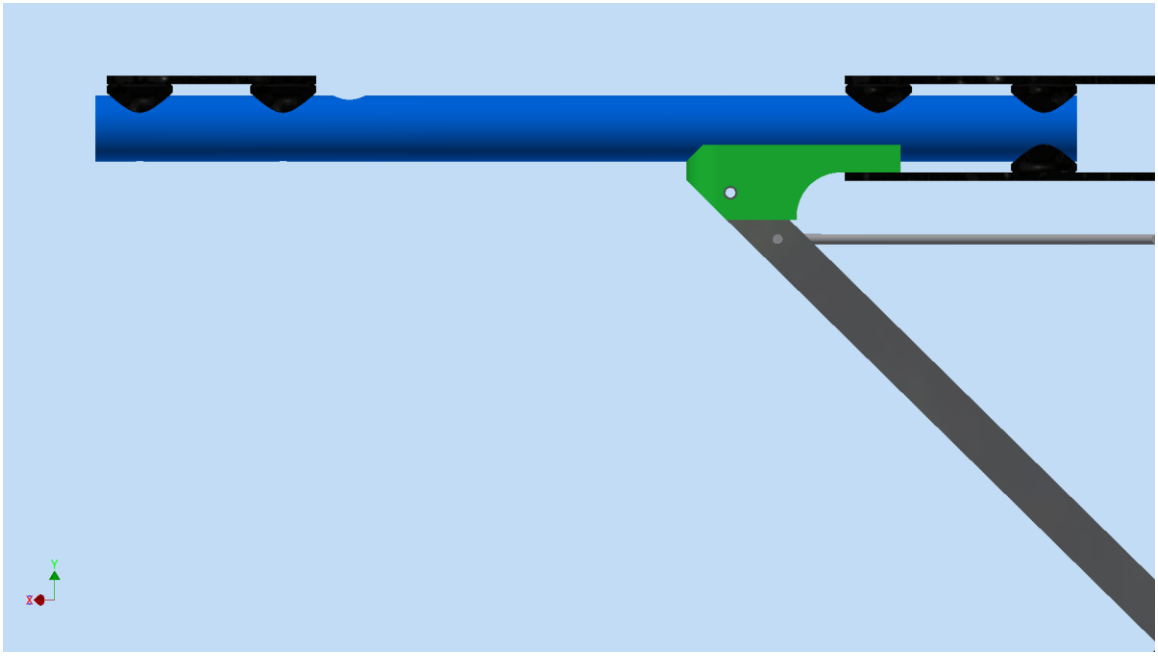

Figure 9: Side view of single landing gear – Position 2.

To allow for the L-shaped extrusion to rotate in an enclosure, a special hinge was designed. This is specific to this implementation and other landing gear may have slightly

different designs for the hinge component. This hinge is shown in Position 1, between Positions 1 and 2, and Position 2 in Figure 10, Figure 11, and Figure 12 respectively. Figure 11 is included so as to clarify what the transient motion looks like in this design. As can be seen in Figure 12, the shape of the hinge is such that in Position 2 the hinge does not obstruct a straight path for the ring to follow when it is sliding against the leg of the aircraft.

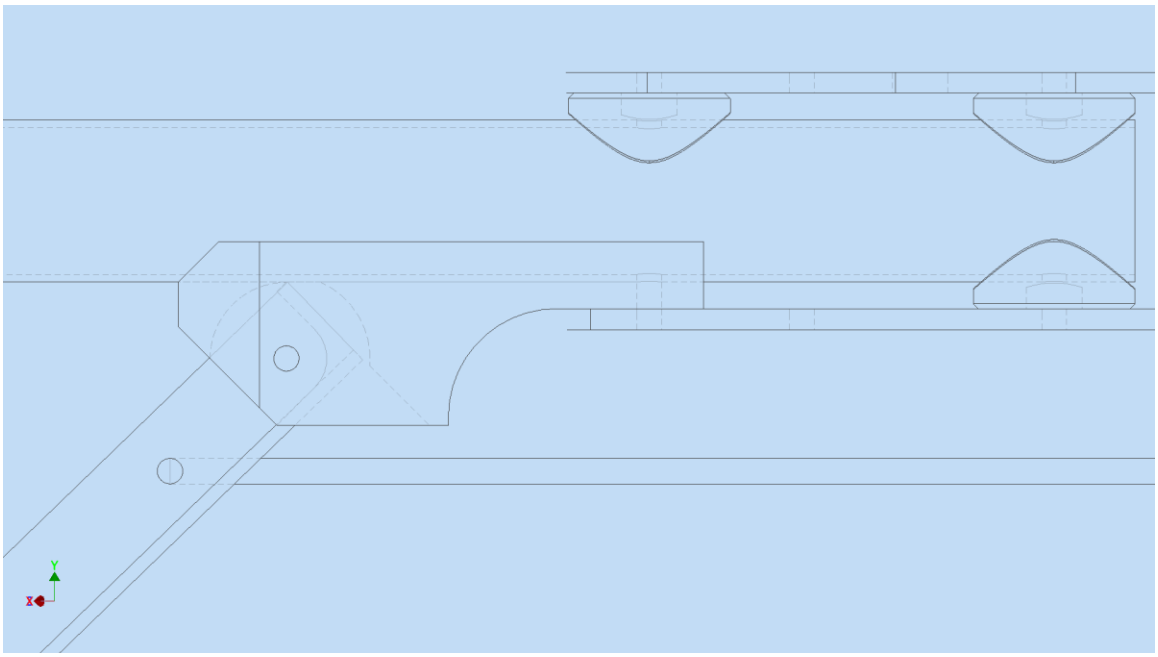

Figure 10: Wireframe drawing of leg hinge – Position 1.

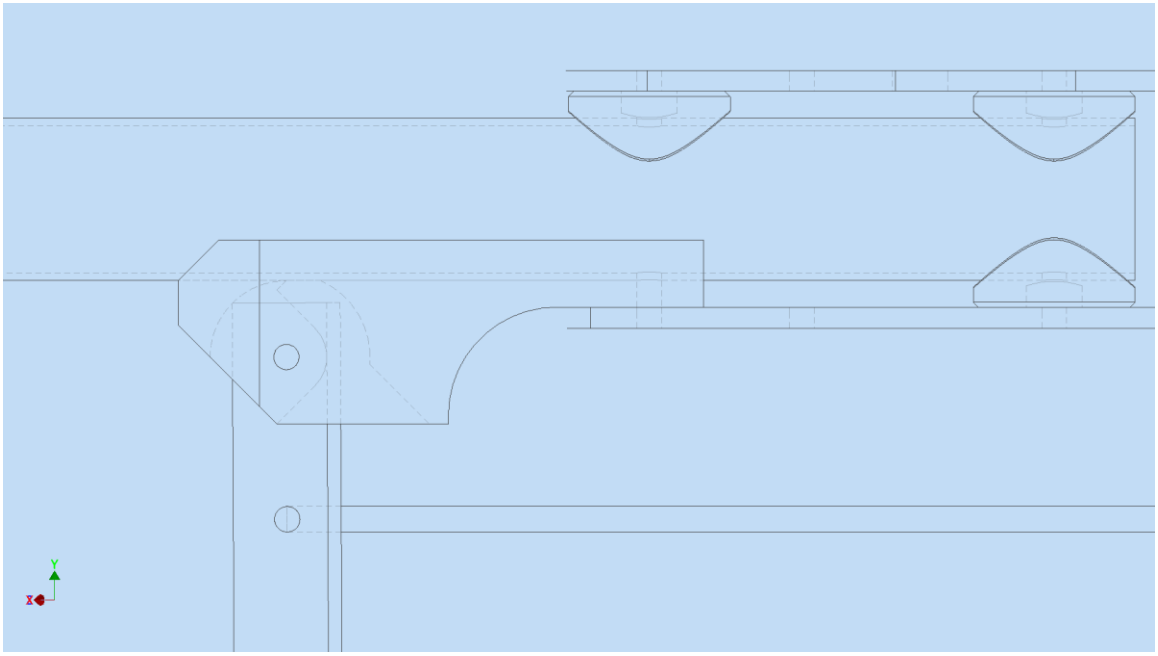

Figure 11: Wireframe drawing of leg hinge – Transient between Position 1 and 2.

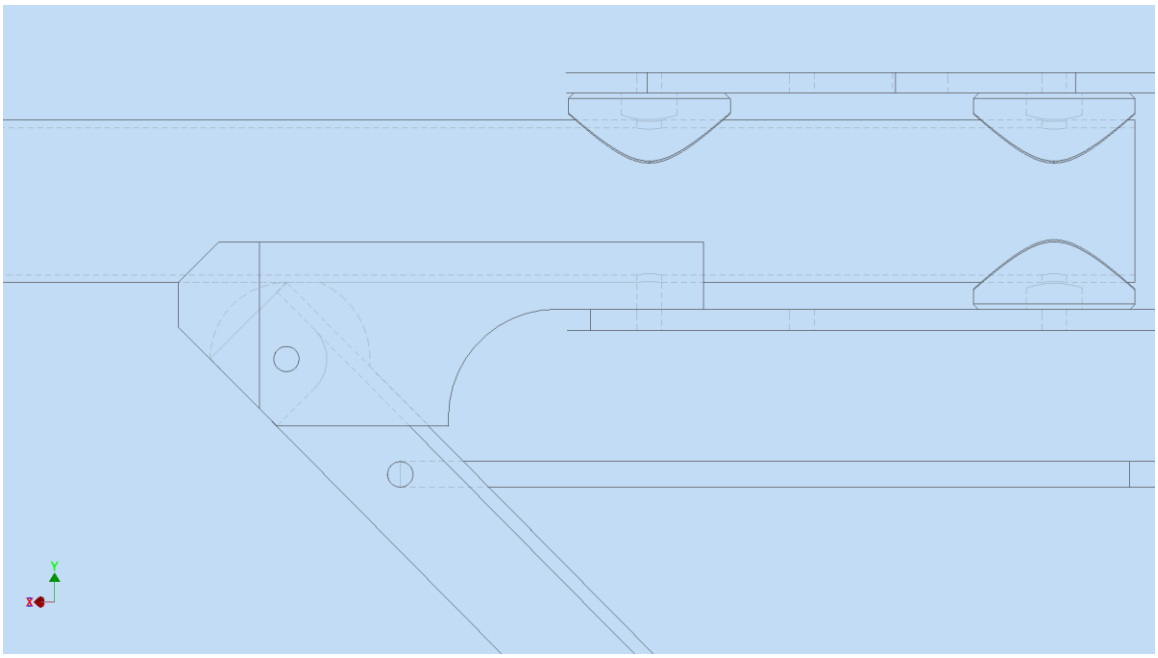

Figure 12: Wireframe drawing of leg hinge – Position 2.

As can be seen in Figure 10 and Figure 12, the L-extrusion is able to fit in the hinge and at the extremes of Positions 1 and 2 the leg comes in contact with surfaces of the hinge as to mechanically stop it from rotating further. A closeup of the hinge is shown below in Figure 13. The surfaces marked 1 and 2 are the surfaces that the leg contacts when in Positions 1 and 2 respectively.

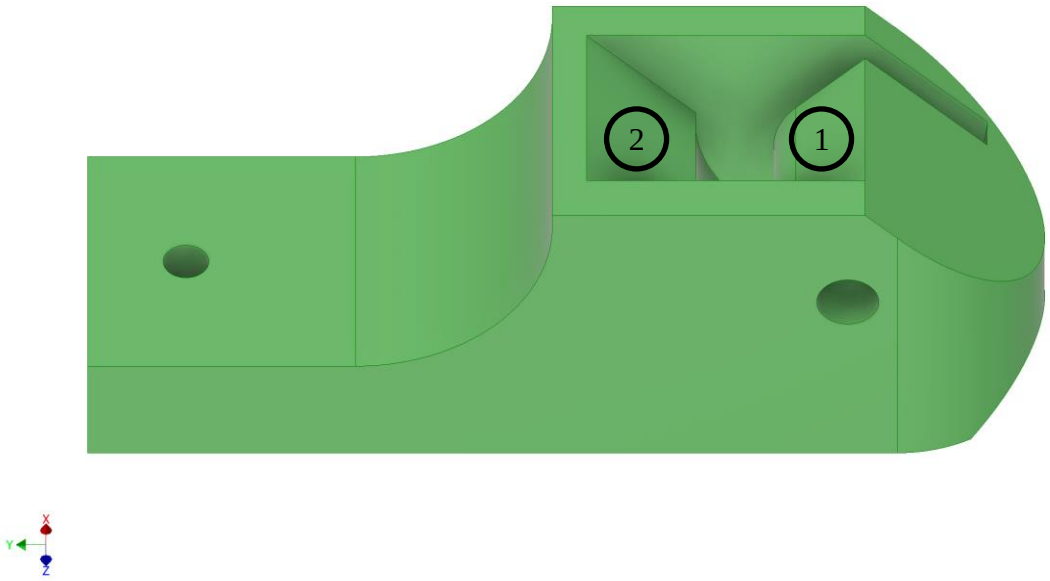

Figure 13: Close-up of hinge design.

Shown below in Figure 14 is the linkage system used to allow the use of a single motor for actuation of the aircraft legs. Attached to the servo motor is a four-way servo arm. Attached to the arm are pushrods that go to each leg. The use of a single motor to actuate the legs is beneficial as there would otherwise be a separate motor attached to each leg, thereby complicating the device mechanically. The use of one motor means that all of the legs actuate in synchronization with each other. Finally, when the legs are in Position 1 with a payload, the force on opposite push rods act against each other instead of applying torque on the motor. Therefore, the device does not require significant electrical power to the motor to keep the legs from being force inwards.

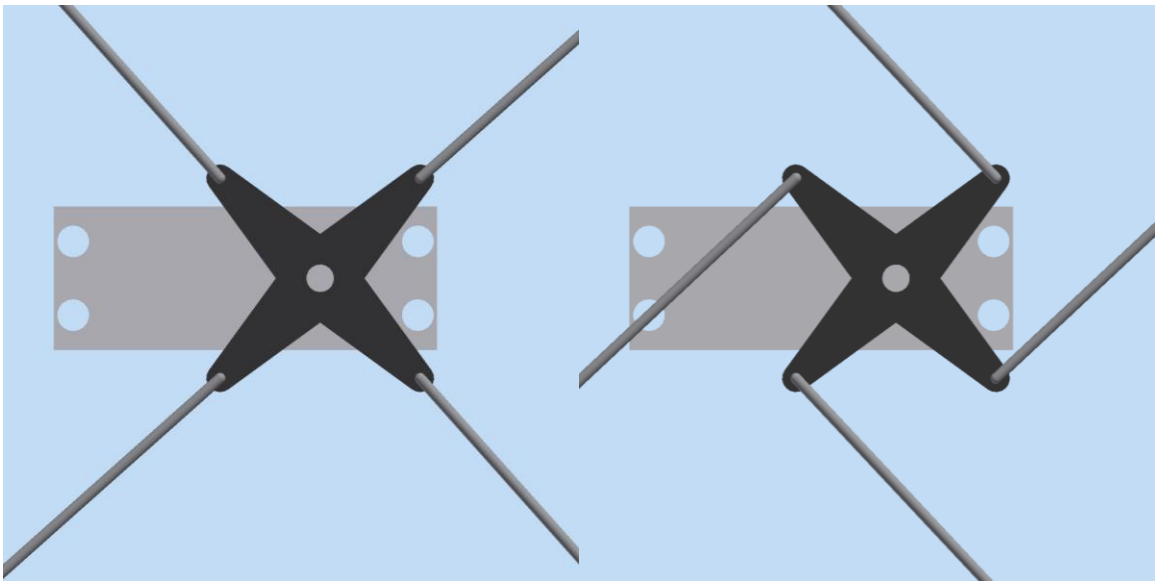

Figure 14: Actuator linkage system - Positions 1 (Left) and 2 (Right).

The docking receptacle that the aircraft lands in can be various shapes (*n*-sides for *n*-legs) if it is desired for the aircraft to be forced into a specific yaw angle relative to the ring. As the yaw did not need to be passively controlled in this implementation, a circular ring was used. The primary requirement is for the inner diameter of the ring to be the same as the distance between opposite hinges. Figure 15 shows the design of the ring prototyped in this project. It should be noted that, while the ring is circular and will not cause the aircraft to be pushed to a certain yaw angle, the yaw angle will not change once the aircraft has docked. This is due to the friction caused by the actuated legs which is great enough to prevent rotation of the aircraft relative to the ring under normal flight loads. This ring was made using a 3ft long aluminum extrusion that was curved into the ring. The diameter of this ring is therefore 11.46in.

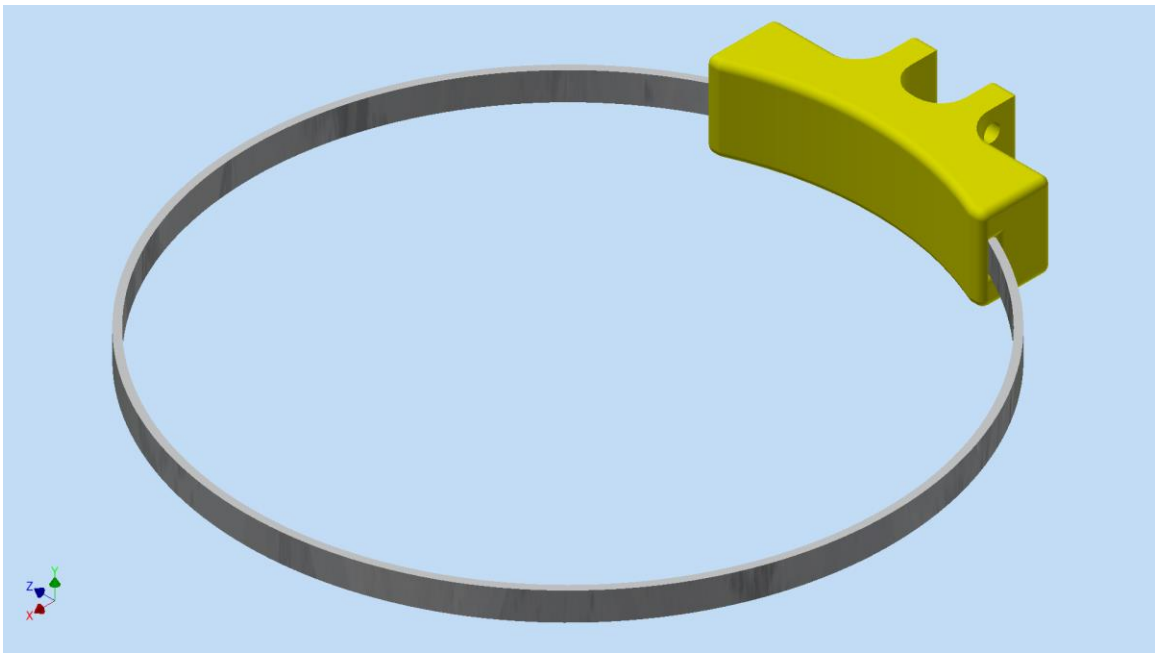

Figure 15: Docking ring design used in this project.

4.2.2 Camera Gimbal

The camera gimbal necessary for the control algorithm was constructed using 3D printed components and digital micro servos. The 3D printed parts are simply for connecting the servos to the camera. It should be noted that in this implementation of the camera gimbal, the tilt is in the frame of the pan. This does mean that they are not fully independent angles, but the angles being used here are small enough when they are close to the zero so that they can be assumed to be space-fixed rotations. A photograph of this is shown below in Figure 16. Wires connecting the camera to the microcontroller were removed for visual clarity.

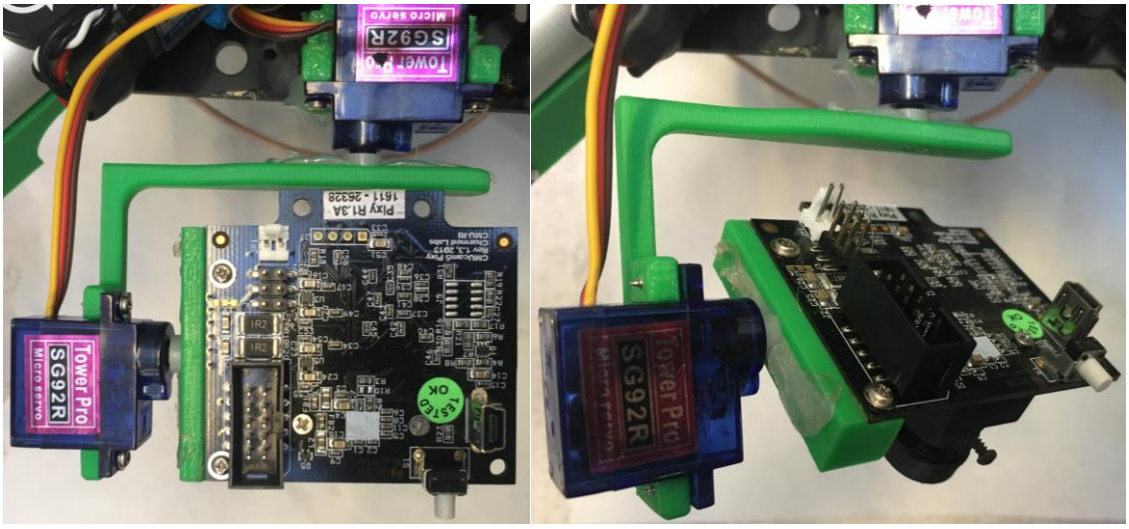

Figure 16: Camera gimbal.

It should be noted that all components that have been discussed so far (excluding the ring until attached) are onboard the aircraft. The inclusion of these components to the system shows an increase in mass of 305g over the standard Elev-8 platform as implemented in this project. Not including the backup flight controller for emergency takeovers (a system that is typically not necessary), the increase in mass is approximately 223g. This is well within the rated lifting capacity of this aircraft (approximately 1.4kg) and includes all systems necessary for precision landing, leg actuation and docking.

4.2.3 Beacon Enclosure

A component that is sold by IR-Lock is an enclosure for the PCB infrared beacon which is an acrylic enclosure that improves performance in outdoor lighting. While this component is pre-existing as a commercial product, it was unavailable (out of stock) when needed in this project. Therefore, a custom one was made by taking measurements of the beacon and laser cutting 1/8th inch medium density fibreboard (MDF). The part was then

painted matte black to maximize the machine vision performance as this maximizes contrast and minimizes glare. This component can be seen in Figure 17 and is photographed in Figure 18. This can be compared to the commercial product shown in Figure 19.

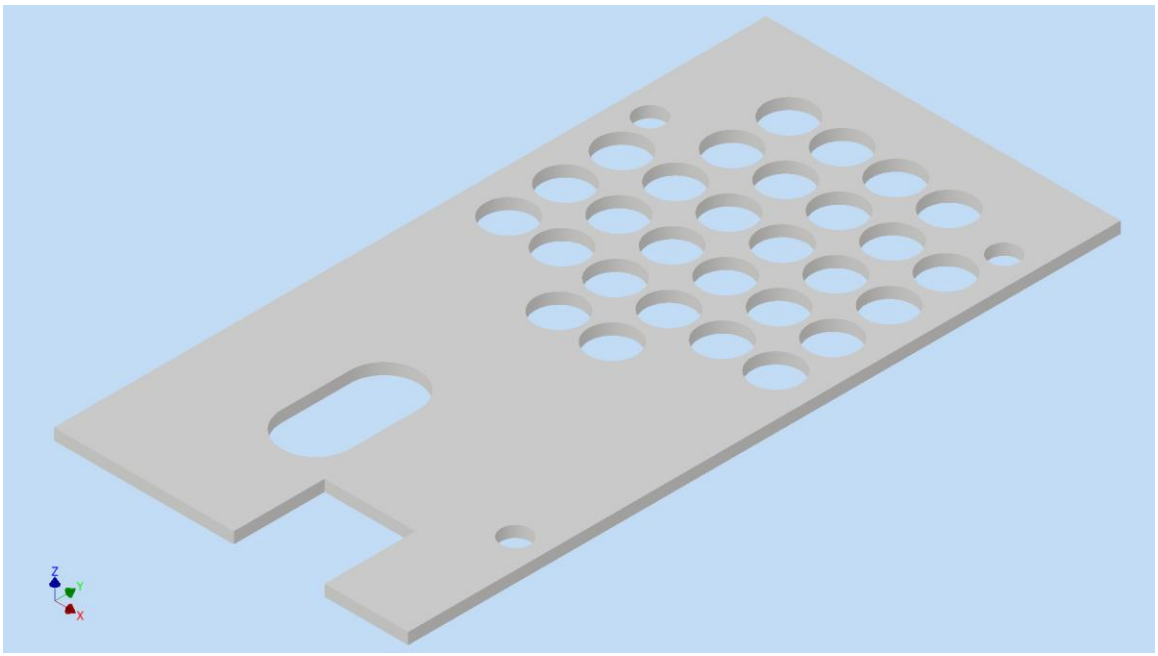

Figure 17: Beacon enclosure CAD.

Figure 18: Manufactured enclosure.

Figure 19: IR-Lock commercial enclosure. (Case for MarkOne Beacon, 2017)

4.3 Full System Images

This section contains photographs of the implemented landing and attachment mechanism. Shown in Figure 20 is the result of all modifications made to the Elev-8 platform. These physical changes include the new landing gear, the camera on gimbal, and the backup flight controller for safety.

Figure 20: Elev-8 with modifications made for this project.

Shown in Figure 21 and Figure 22 is a view of the hinge developed in both Positions 1 and 2, respectively. To achieve this, the pushrod (as pictured) is actuated by the standard servo motor. This actuator is shown in Positions 1 and 2 in Figure 23 and Figure 24 respectively.

When the docking ring is attached to a payload, gravity will be acting on this such that the ring will have downward force on the landing gear. These forces would cause the legs to be forced inwards towards Position 2. As is seen in Figure 23, the arms of the servo for actuating the legs are nearly colinear with the pushrods when in Position 1. This is greatly beneficial as the force along the pushrod generated by the torque applied to the

landing gear in Position 1 have a very small moment arm to the servo. This means that the holding torque of the motor remains low even when the payload force on the legs is high.

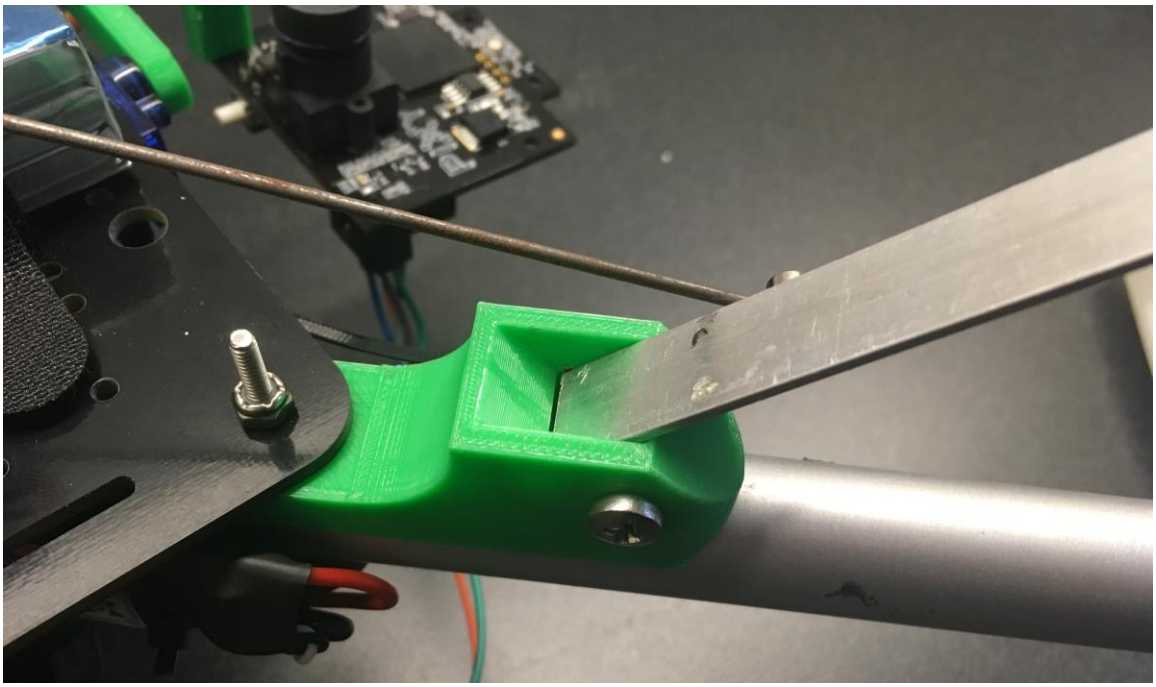

Figure 21: Photo of single leg in Position 1 (photo from below for visual clarity).

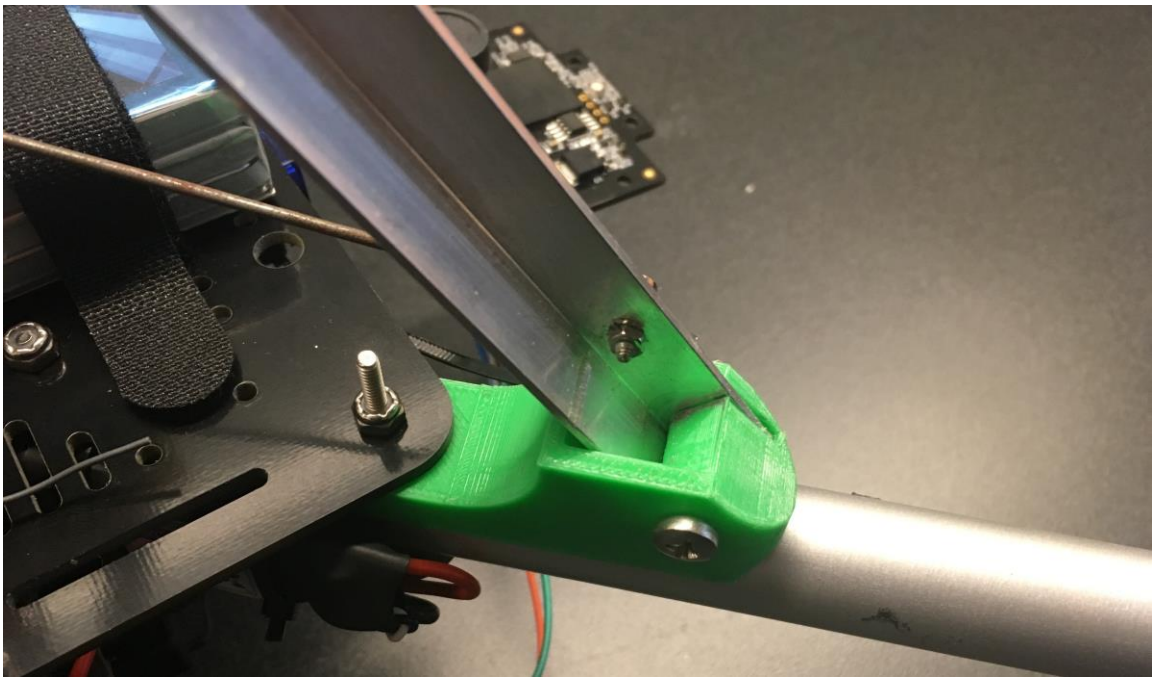

Figure 22: Photo of single leg in Position 2 (photo from below for visual clarity).

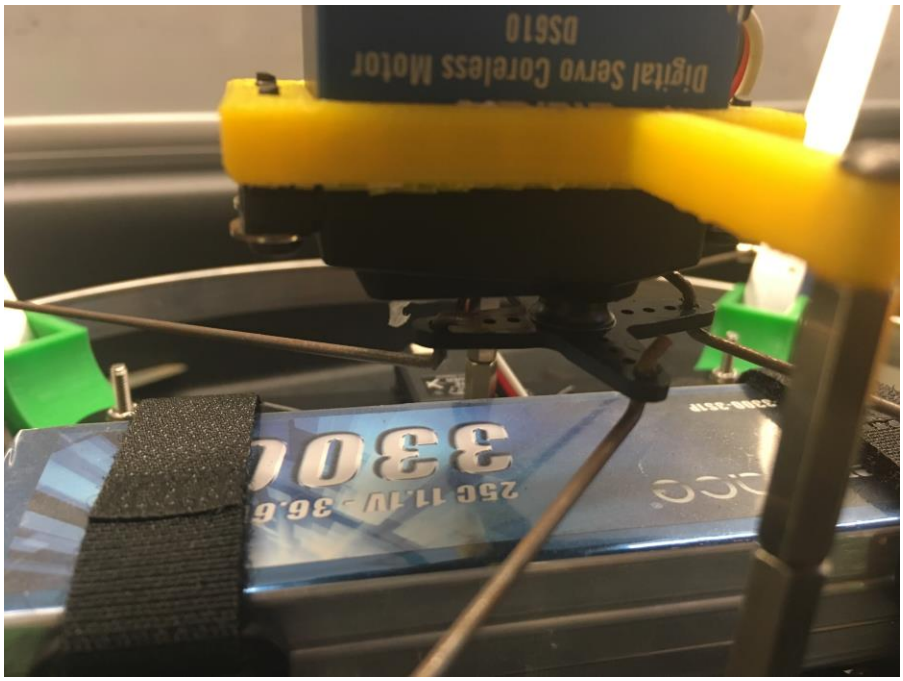

Figure 23: Landing gear actuating servo - Position 1.

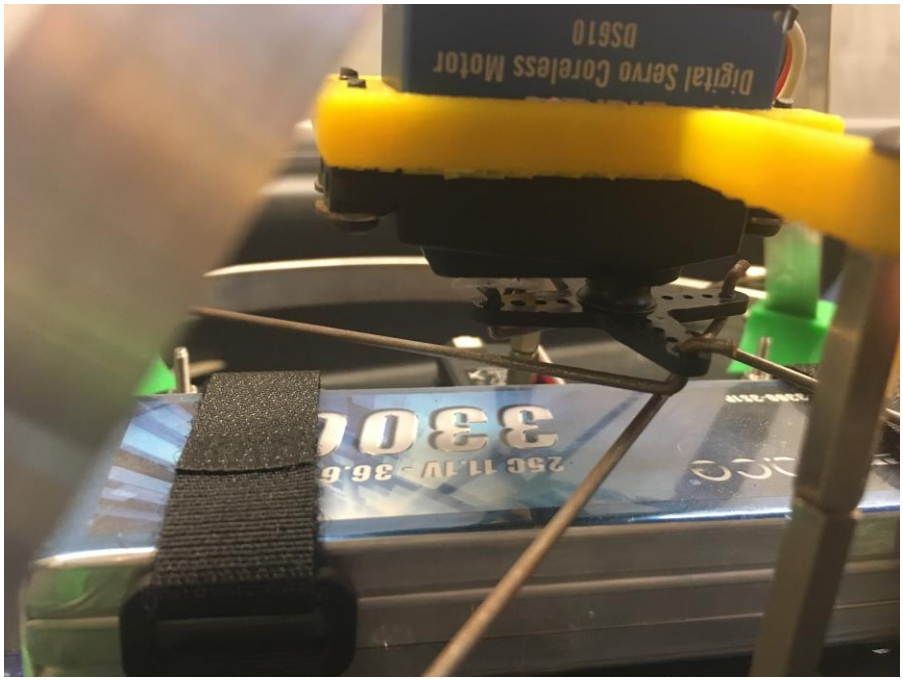

Figure 24: Landing gear actuating servo - Position 2.

For the ring to be locked in place, the legs must move from Position 2 to Position 1. A close up of the way in which the legs lock the ring in place is shown below in Figure 25 and Figure 26. Here, it can be clearly seen that even when the ring does not settle perfectly in place, the actuation from Position 2 to Position 1 provides the final shift, forcing the ring into the fully locked position. Once positioned like this, the ring has no room to rotate along the roll and pitch axes and the friction is great enough that it is difficult to rotate along the yaw axis.

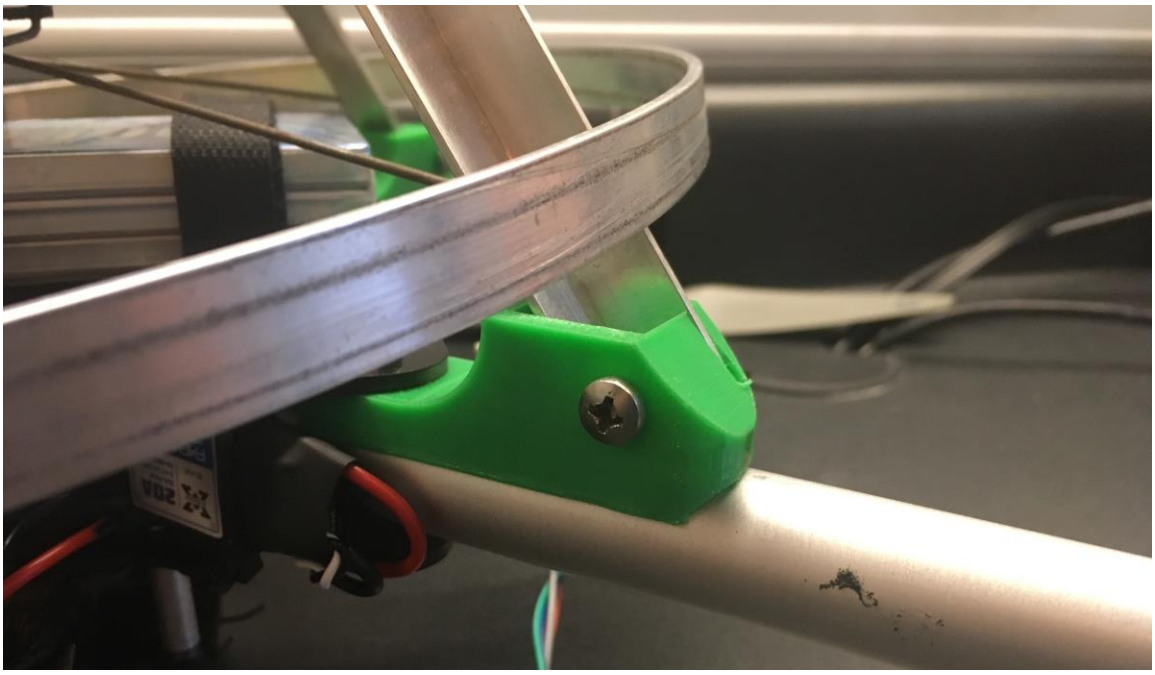

Figure 25: Ring locking mechanism closeup - Position 2.

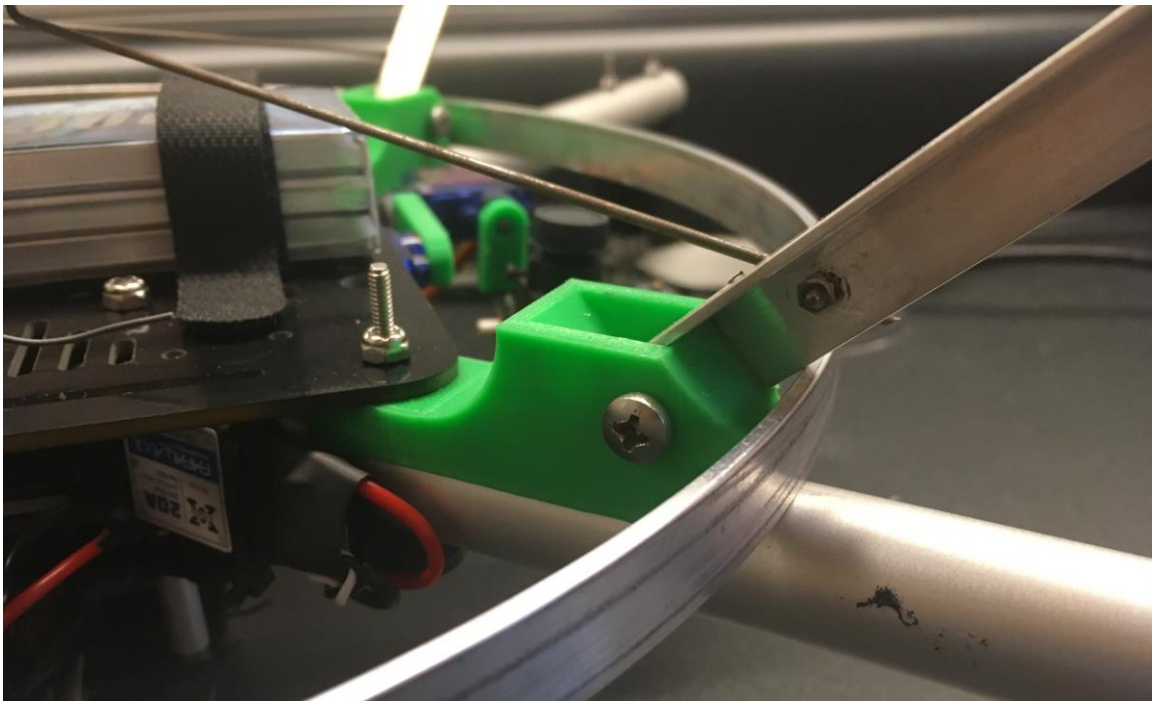

Figure 26: Ring locking mechanism closeup - Position 1.

Figure 27 and Figure 28 have been provided to show landing gear in both positions.

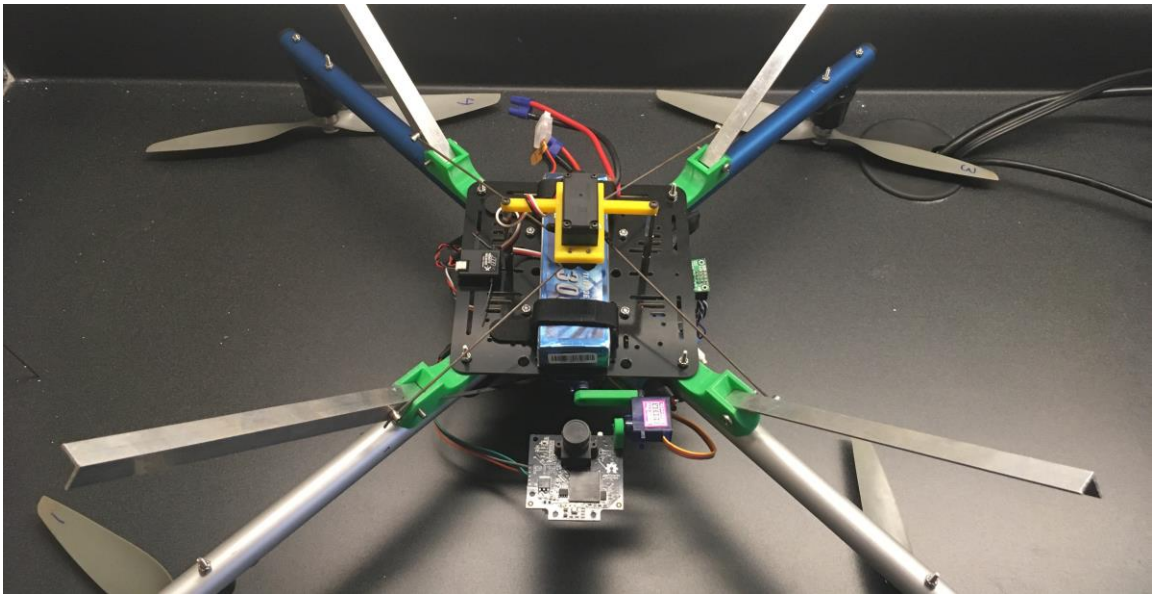

Figure 27: Bottom view of Position 1.

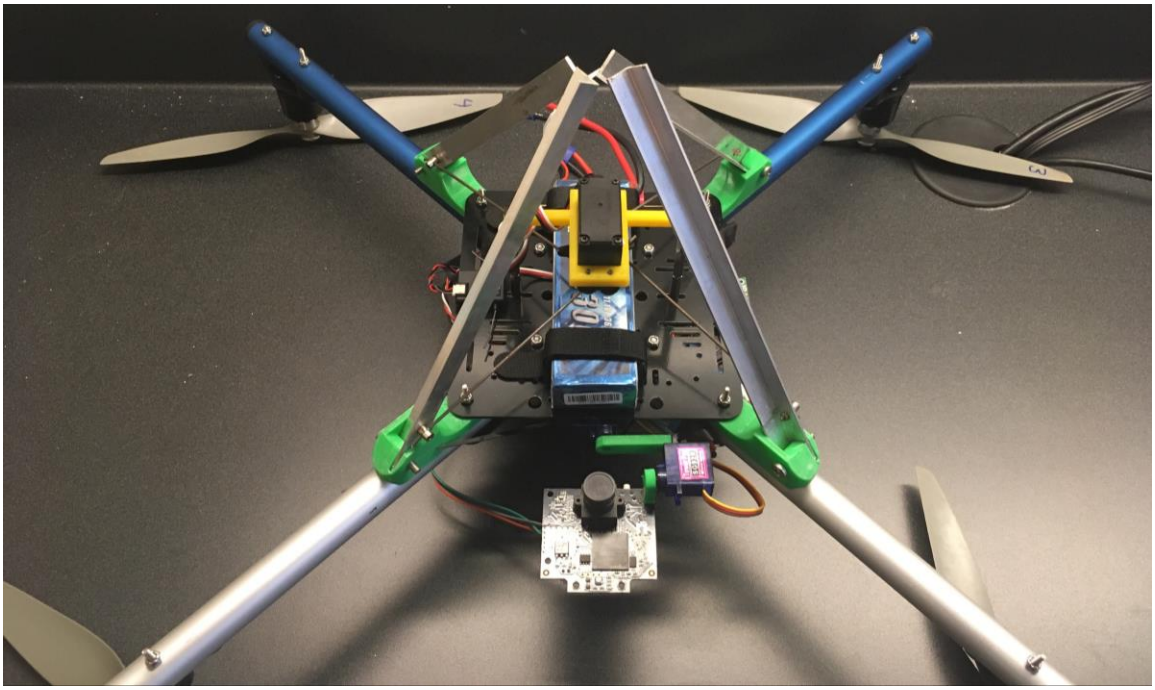

Figure 28: Bottom view of Position 2.

Figure 29, Figure 30 and Figure 31 illustrate the process of precision passive positioning and attachment. These were shown to work well in practice as shown in Figure 32.

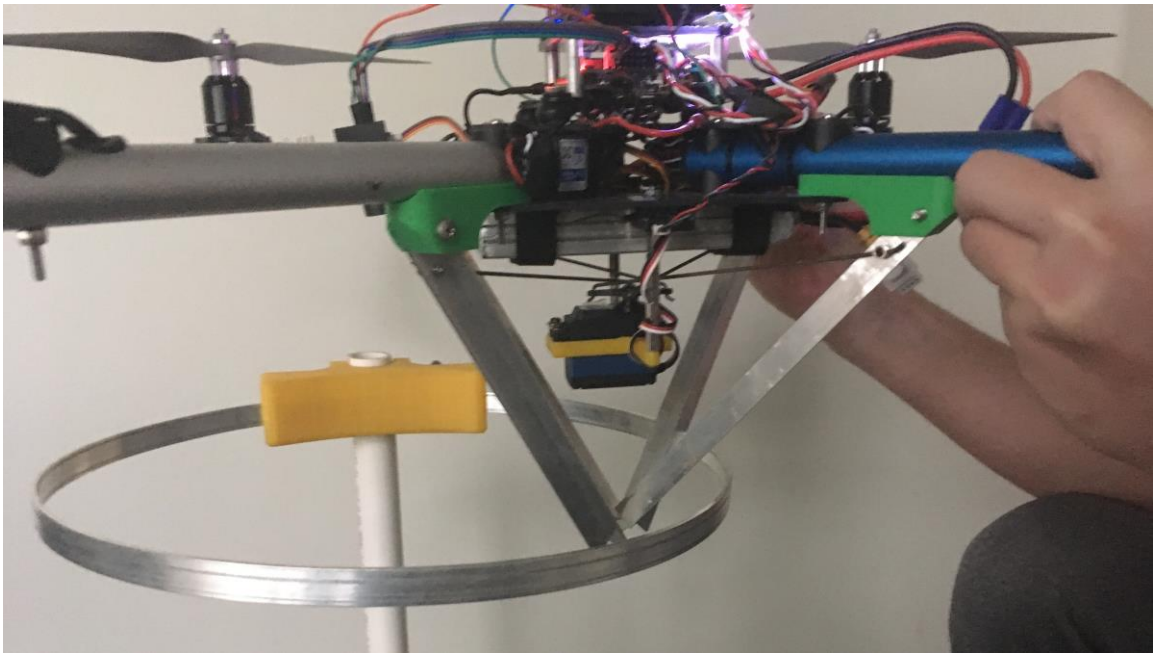

Figure 29: Entry of the vehicle into the dock.

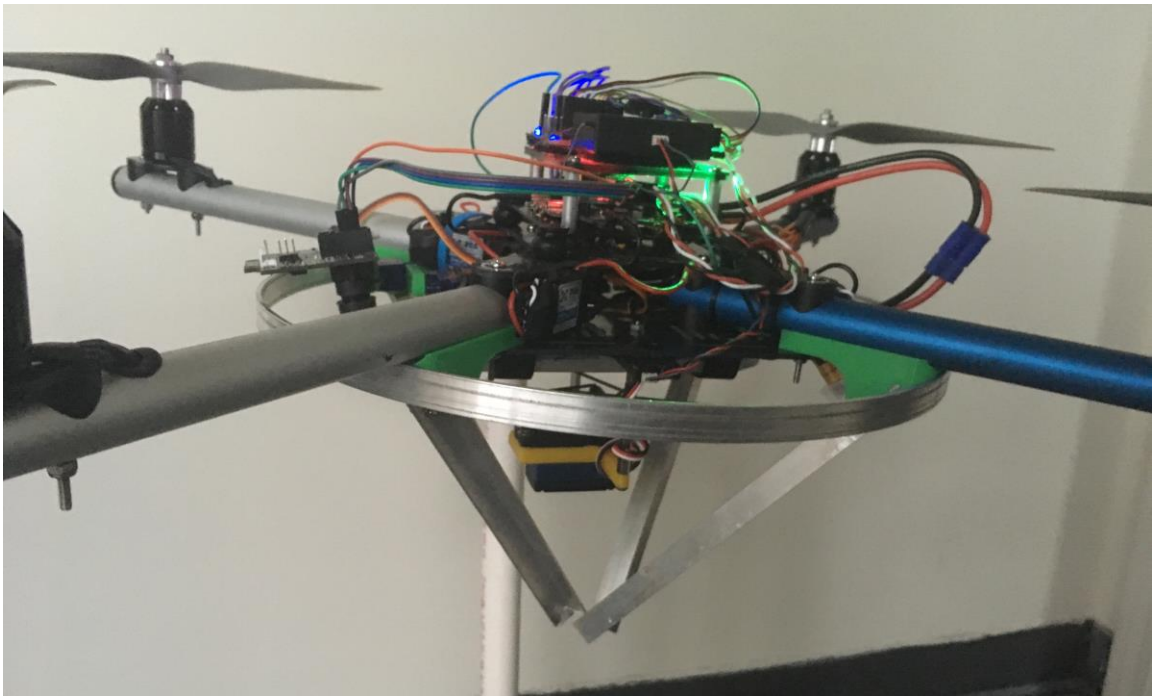

Figure 30: Vehicle settled into dock.

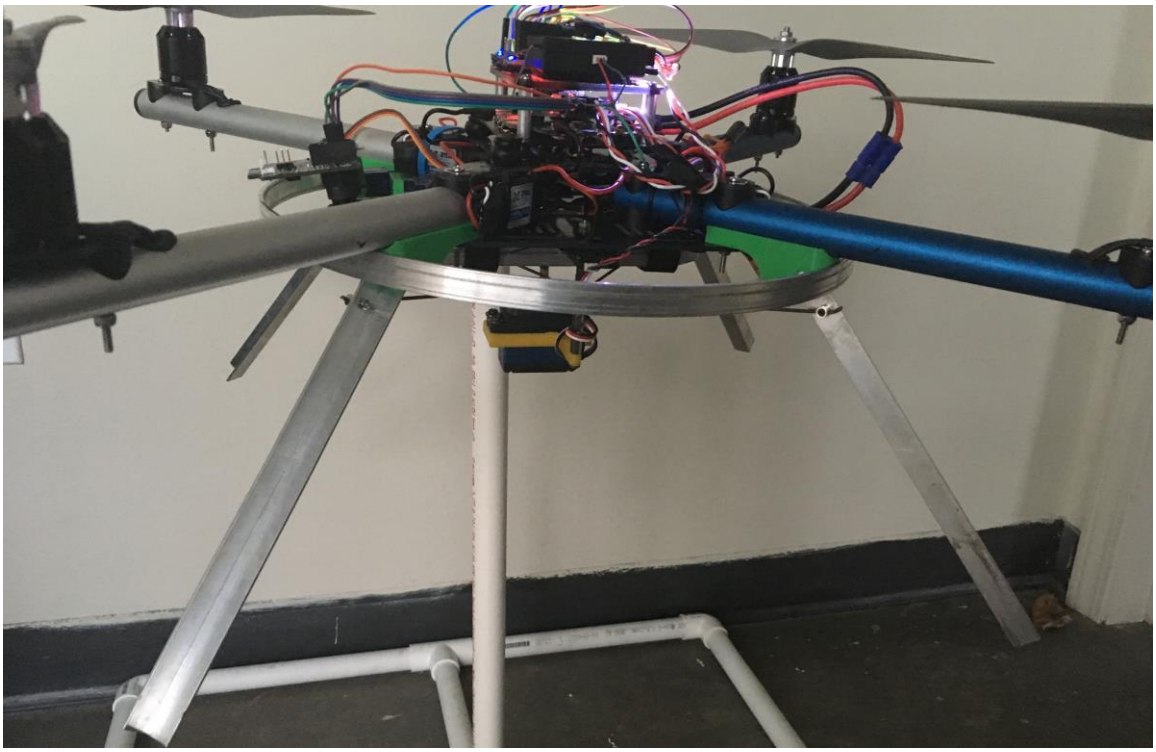

Figure 31: Vehicle attached to dock.

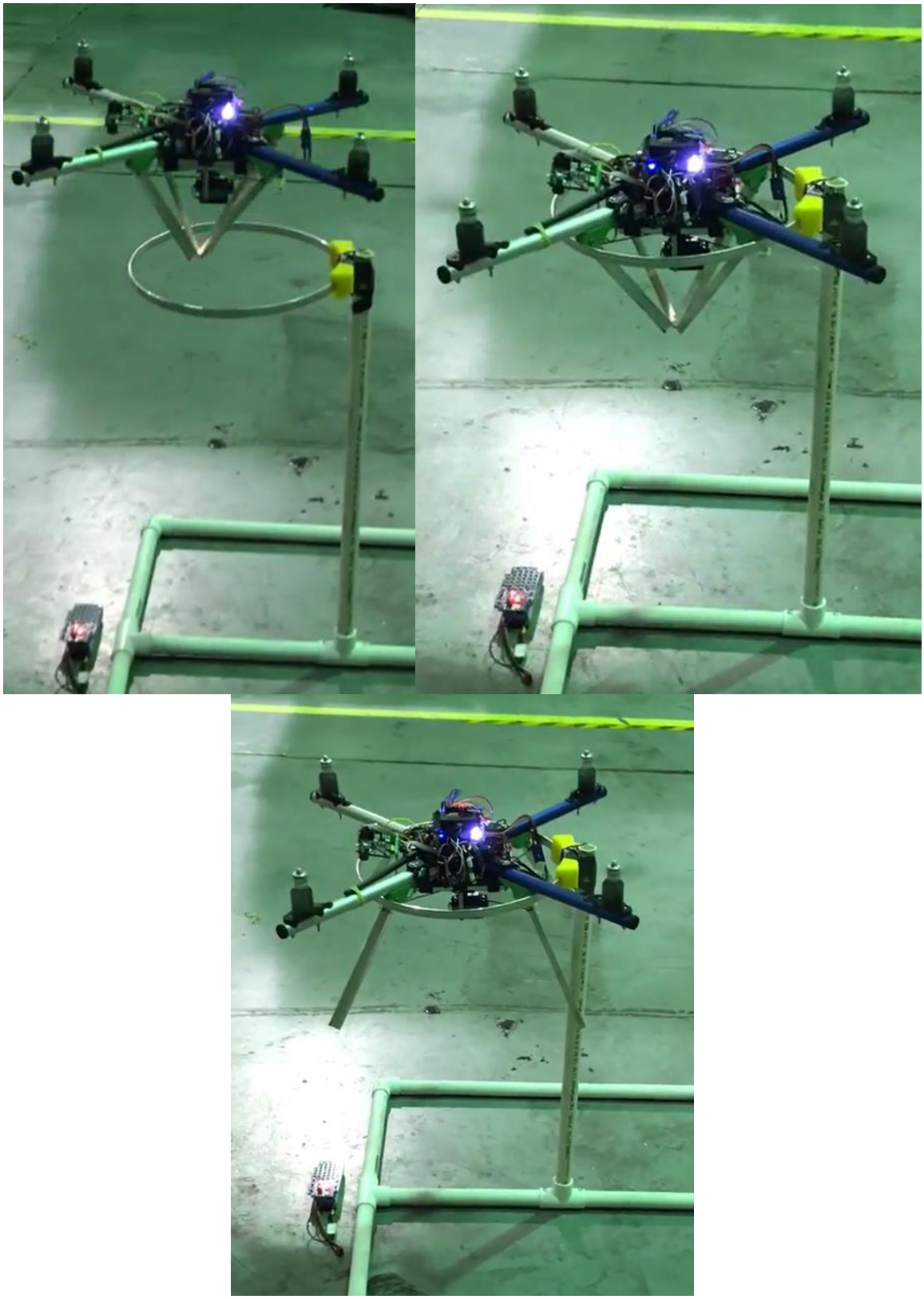

Figure 32: Flight experiment demonstrating successful autonomous docking.

4.4 Algorithm Implementation

This section provides information on the embedded software that was implemented for the autonomous control.

4.4.1 Parallax Microcontroller Implementation

The Parallax microcontroller is wired such that the radio input goes into the DSM pin-header provided on the Rev-B platform. The motor PWM outputs are connected through the multiplexer to the electronic speed controllers. Various GPIO pins (interchangeable) are connected to the leg actuating servo, and Arduino serial line. The code on the microcontroller is a variant of the code provided by Parallax written by Jason Dorie. (Dorie, 2017) The control law is written to a new cog (core) of the microcontroller where it is processed separately. The pre-existing code on the other cores was modified to read these commanded roll/pitch angles and desired altitude to achieve autonomous flight.

4.4.2 Arduino Microcontroller Implementation

The Pixy was connected into the ICSP port of the Arduino microcontroller. The Arduino 5 volt in, ground, and TX (transmit) pin were connected to the Parallax 5 volt line, ground and a single GPIO pin respectively. The code used on board the Arduino microcontroller is a variant of the pantilt.ico file provided by CMU labs.

4.4.3 Full Algorithm Implementation

The algorithm was implemented on the hardware listed above. Figure 33 is a complete flowchart of the flow of logic for this precision guidance maneuvering technique.

Each microprocessor runs its own loop, passing information that the next microcontroller waits for, processes, and repeats. The Pixy provides to the Arduino the position of the beacon in the frame of the camera. The Arduino calculates the correct angles for the gimbals to point the camera at the beacon. The Parallax Elev-8 calculates the desired vehicle roll/pitch angles and desired altitude needed for autonomous control.

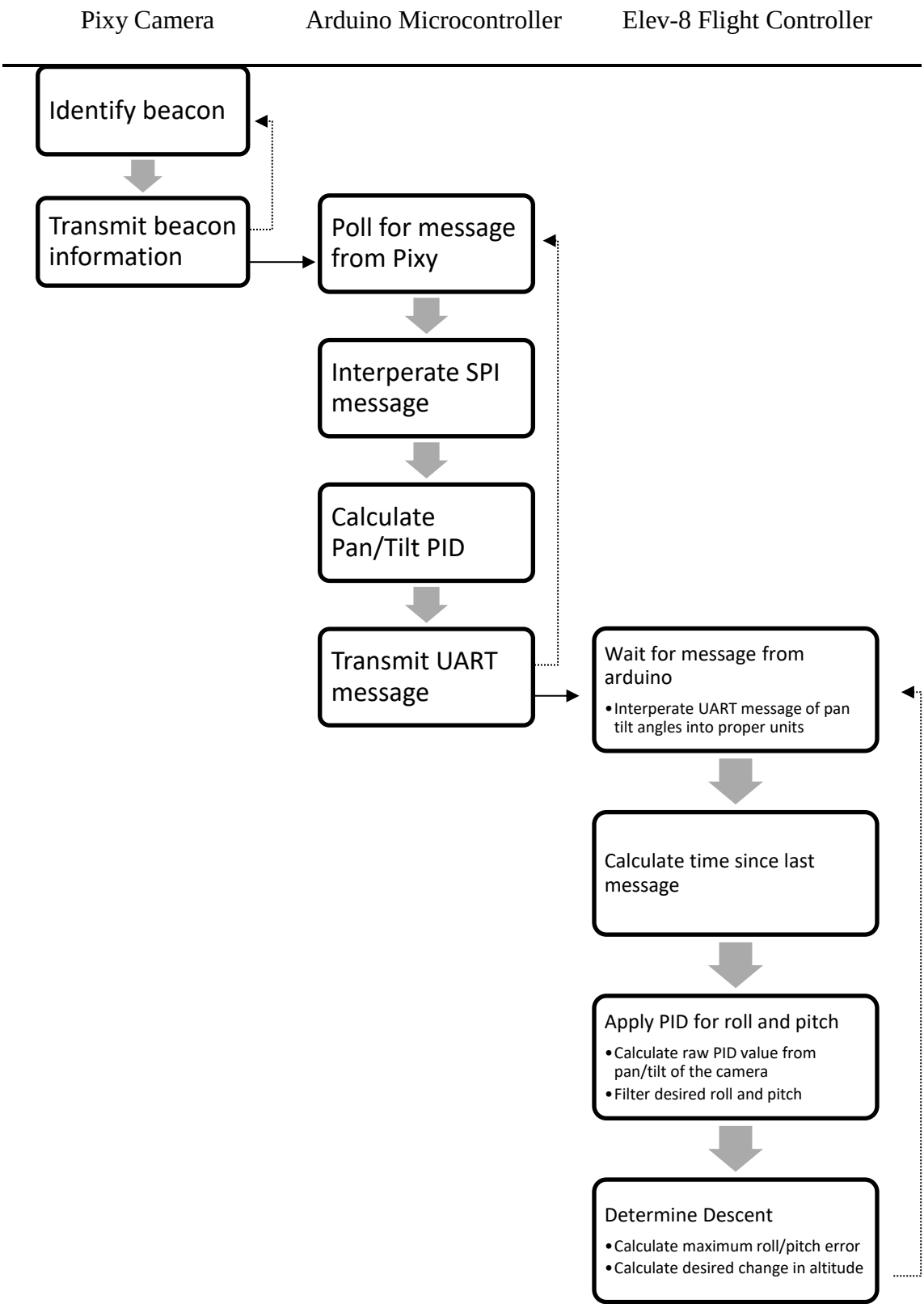

Figure 33: Flow of algorithm through components.

4.5 Tuning Methods

The primary method for tuning both the PID loops for controlling camera tracking and aircraft control was a variant of Zeigler-Nichols tuning. In both cases, the proportional, integral and derivative gains were all set to zero to start. Then the proportional gain was increased until it seemed to approach the $P_{ultimate}$ where the system becomes marginally unstable. Then the proportional gain was decreased to $0.8P_{ultimate}$ and the derivative gain slowly increased until the system showed desirable performance. The camera tracking did not require integral gain. In indoor conditions the aircraft control did not require integral control, but integral control was added for outdoor flying to compensate for wind. As Zeigler-Nichols contains "rule-of-thumb" approximations, small modifications were made to the PID values to improve performance further based on data gathered from tests.

CHAPTER 5. RESULTS AND FUTURE IMPROVEMENTS

This project has proven to be successful with reliable performance in both indoor and outdoor flight tests. The results of this project suggest the methods presented are a viable solution for low overhead and low cost precision docking. With this system, an aircraft can dock at a home location or at a payload. The system is modular enough to allow for multiple docks to be attached to larger payloads for cooperative lifting. Presented in this chapter are the quantitative results of this system from indoor and outdoor testing. Additionally, there are recommendations for future versions of this system based on what was learned from this prototype.

5.1 Flight Test Results

This section will provide results from flight experiments. First discussed will be the performance of the camera detection rate of the beacon. Next will be the performance of the gimbal tracking the beacon. Finally, a discussion of the aircraft control including roll/pitch commands and desired altitude output will be provided.

5.1.1 Pixy Camera Performance

The camera used in this project has an update rate of 50Hz. According to IR-Lock, this camera is supposed to reliably detect the beacon at a range as far as 20m. These values are more than sufficient for the scope of this project. As shown in Figure 34, it was found that these claims are true in ideal conditions.

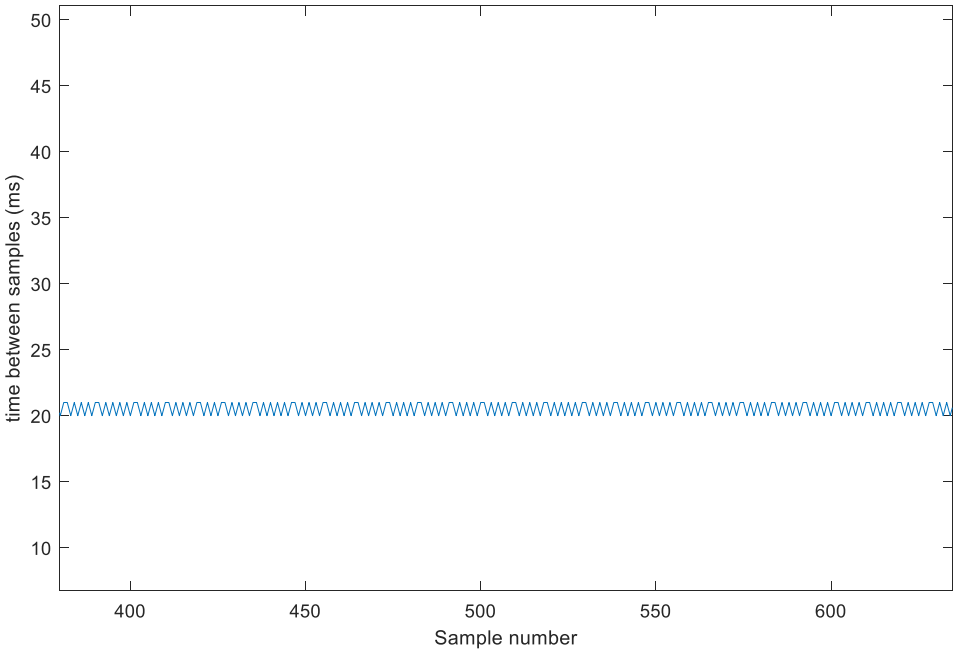

Figure 34: Time between captures of beacon – Ideal conditions.

The real challenge occurs when using this device outdoors where sunlight interferes with the detection rate. As discussed earlier, IR-Lock sells a beacon enclosure that is supposed to improve outdoor performance. Without any enclosure, detection suffers greatly to the point where the time between updates is on the order of hundreds of milliseconds. This greatly reduces the ability for the aircraft to apply its algorithm effectively. As the official enclosure product was unavailable to buy when needed, a similar enclosure was made. As expected, this enclosure was found to improve the performance. An example of the performance outdoors is shown below in Figure 35. Notice that all detections occur at multiples of 20ms, so if there was no detection during one cycle, the camera must wait for the next. Even with this performance being worse than the ideal example given above, this is significantly better than with no enclosure and the detection

rate is fast enough for the control algorithm to be expected to work properly. For the example run below, the average time between detections is 25.31 ms or 39.51Hz.

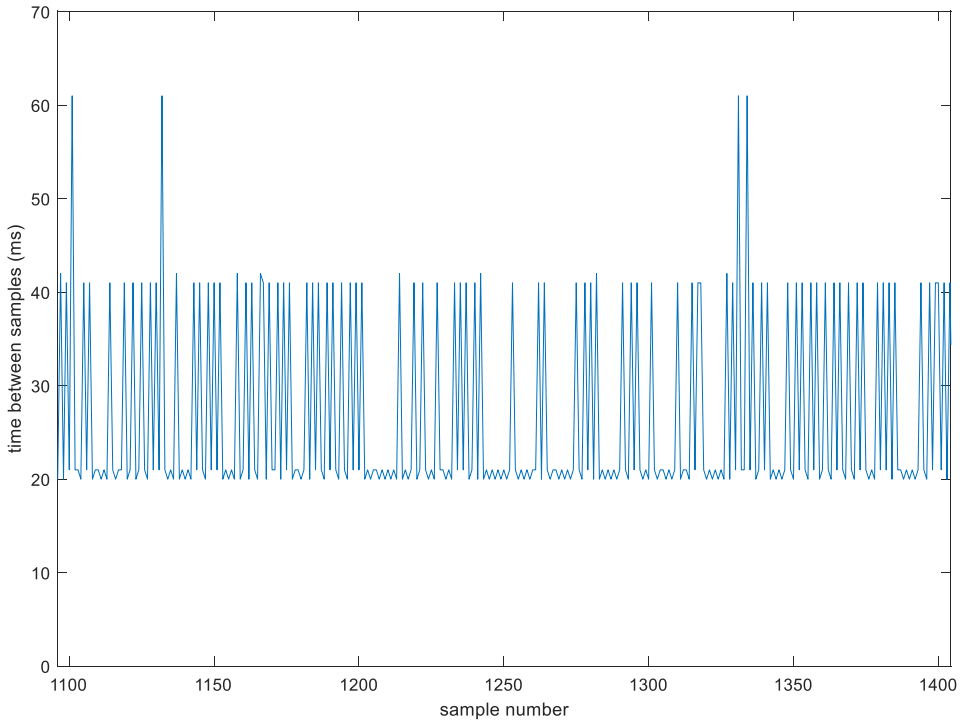

Figure 35: Time between captures – Outdoors.

5.1.2 Camera Tracking

The ability for the camera to track the beacon is very reliable. For both the pan and tilt, the gimbal PID attempts to force the pixel error to zero. The camera has a Δx (associated with pan) output range of about ±160 pixels and a Δy (associated with tilt) output range of about ±100 pixels. If either of these values are exceeded, the camera tracking loses sight of the beacon and would need to re-establish sight of the beacon before the control algorithm could continue. Figure 36 shows Δx and Δy on the frame of the camera during a

successful landing. It is clear that the error is driven near zero for both Δx and Δy and is at little to no risk of losing sight of the beacon through the course of the landing.

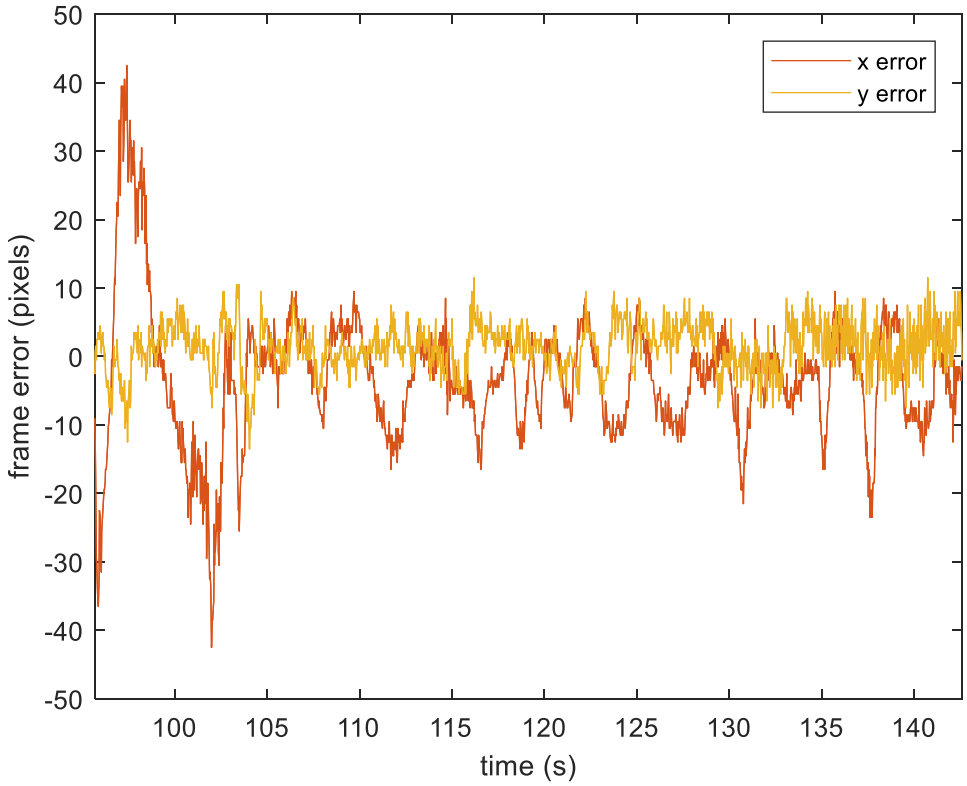

Figure 36: Target error on frame of camera during landing.

The following figures will only look at plots along one dimension of related variables (Δx/pan/roll) for simplification. This pan angle is the result of the PD controller driving the pixel error to zero. The pan angle during this flight example is shown below in Figure 37. The result is comparable for the Δy and associated tilt angle. As is expected, the angle of the camera is inversely related to the frame error. This camera angle is then used as the signal that is processed by the PID loop for controlling the roll of the aircraft. It is useful that this camera angle signal is smooth as a noisy signal would be difficult for the roll derivative controller to manage.

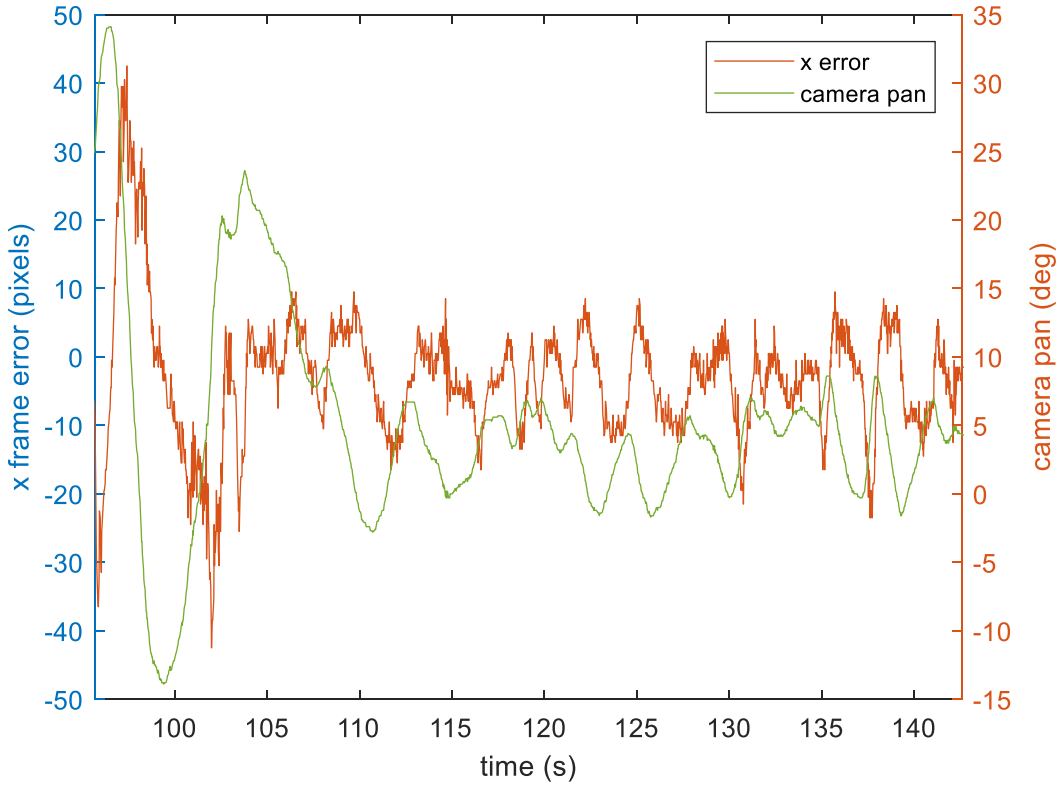

Figure 37: x error and pan angle during flight.

5.1.3 Commanding Roll/Pitch Angle

Observing the camera pan effect on aircraft roll, below in Figure 38 are the results of the desired roll of the aircraft from the pan of the camera.

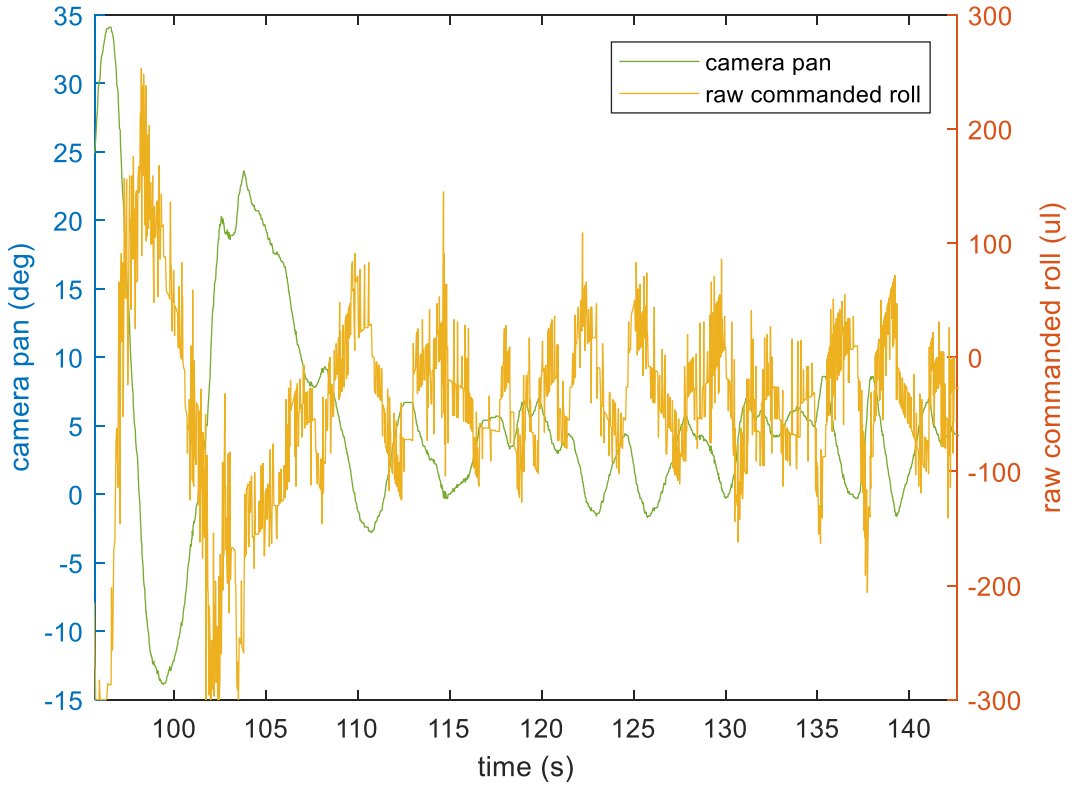

Figure 38: Pan camera angle and raw commanded roll during flight.

As once again expected, the commanded roll is inversely related to the angle of the camera. It would be expected that with such a clean input signal, the output of the PID loop should be clean as well. This was not the case here as the derivative gain for this naturally undamped system is required to be very high. This results in a lot of noise in the derivative control from small changes in signal input.

In indoor conditions, this noisy raw PID output was still able to dock properly. When indoors, the feedback from the camera is at full frequency. As a result, these oscillations in the commanded roll are fast enough that they are beyond the cutoff frequency of the aircraft roll response. These oscillations could still be perceived, though, as the sound coming from the aircraft was noticeably different as compared to manual flight

(low frequency of changing commands). Once outside, the update rate was slowed slightly allowing these oscillations to have greater effect on the flight of the aircraft. The aircraft was then no longer able to fly in a stable fashion.

To compensate for this, a digital low-pass filter was added. This was done using Equation 7

$$y_k = y_{k-1} - \alpha(y_{k-1} - x_k) \tag{7}$$

where y_k is the present filtered output, y_{k-1} is the previous filtered output, x_k is the current raw output and α is the filter strength. The filter strength is a value between 0 (full strength) and 1 (no filter). With this equation a filtered PID output was achieved. An example of this output is shown below in Figure 39. This filtered output, while still somewhat noisy, is much cleaner.

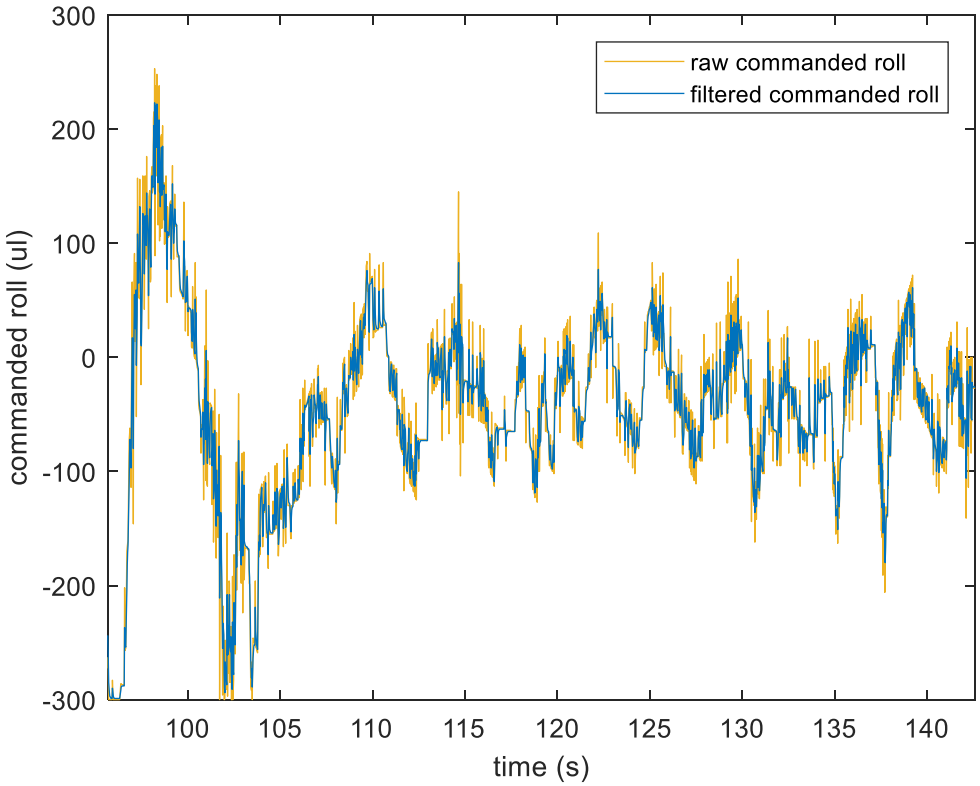

Figure 39: Raw commanded roll and filtered commanded roll.

The results of this filtered command for desired aircraft roll worked far better than the unfiltered. Figure 40 shows the response of the aircraft compared to the commanded with respect to the roll commands. It is clear from this figure that the desired orientation was achieved with minimal lag.

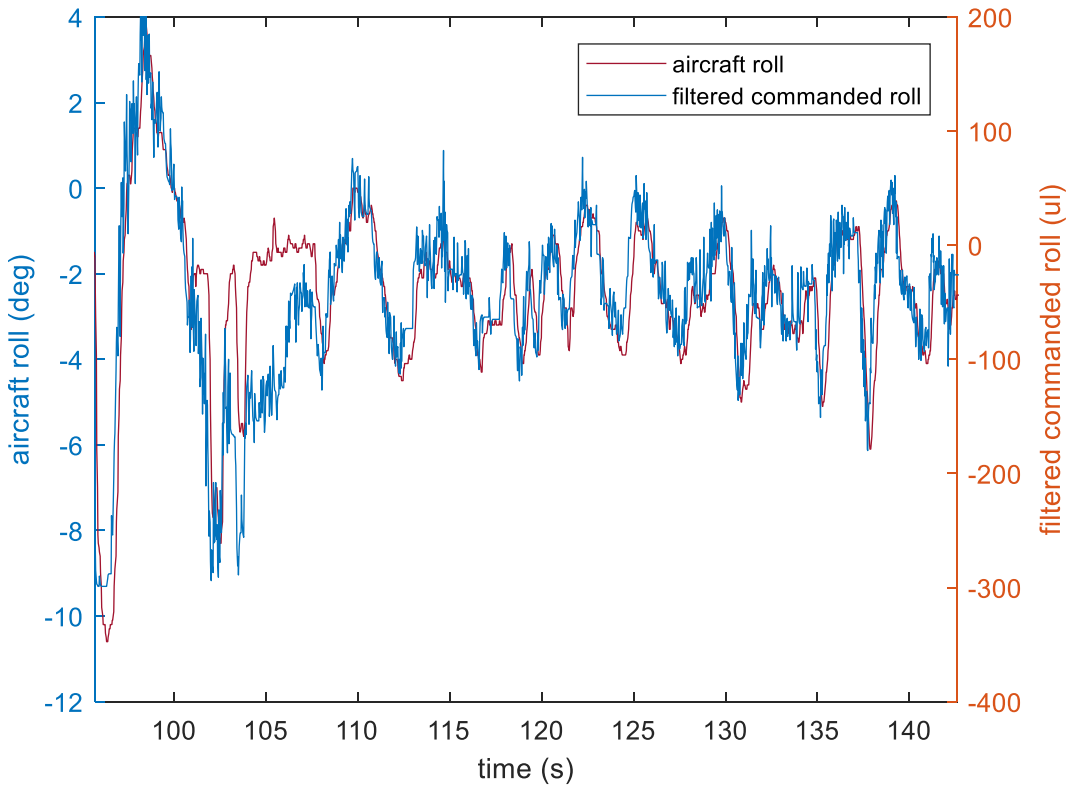

Figure 40: Commanded roll and actual roll.

Figure 41 shows the difference between the angle of the camera pan compared to the roll of the aircraft. This figure shows that the system tends to converge as the system stabilizes over the beacon. Not surprisingly, the camera angle and aircraft angle are inversely related to each other, especially in the latter half of the landing procedure where the system has become relatively steady.

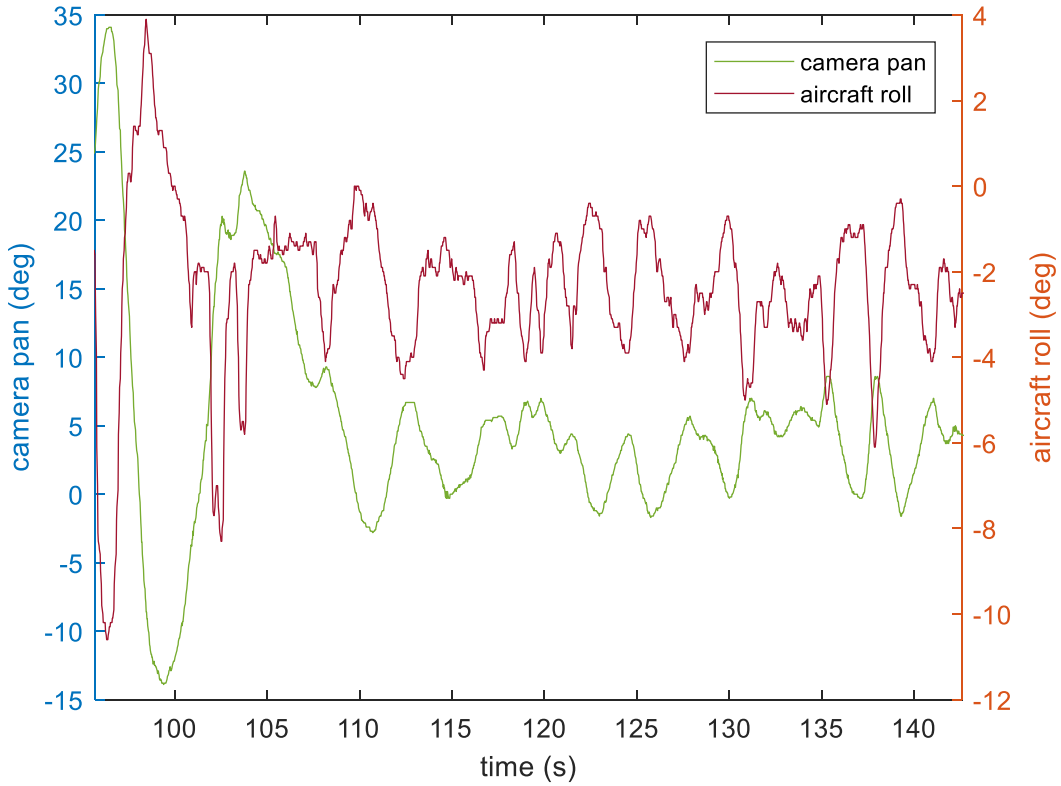

Figure 41: Camera pan and actual aircraft roll.

5.1.4 Altitude Control

As described above, the descent rate is a function of error in the camera angle. The calculation for the error to be used in this function is the maximum of the absolute value of the pan and tilt errors. Figure 42 illustrates the calculated error used. The pan and tilt errors are shown where the maximum of the absolute value of these errors is highlighted with a dotted line. During flight, this dotted line was used to produce a desired change in altitude. An approximation of this desired change of altitude (relative to max error) is shown below in Figure 43. During the actual flight, the desired change of altitude is not approximated. The approximation made in this plot is that the time between acquisitions

of the beacon is 25.31 ms instead of the true value. This approximation was made only for visual clarification as the true plot is very noisy.

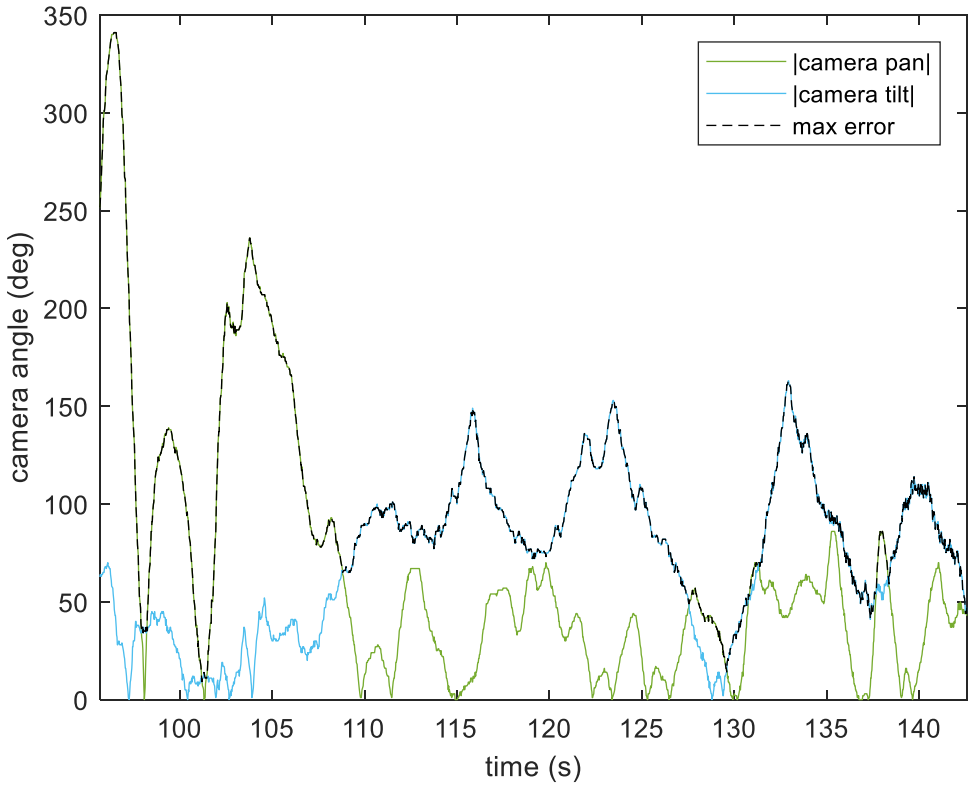

Figure 42: Absolute value of pan and tilt - max error shown with dotted line.

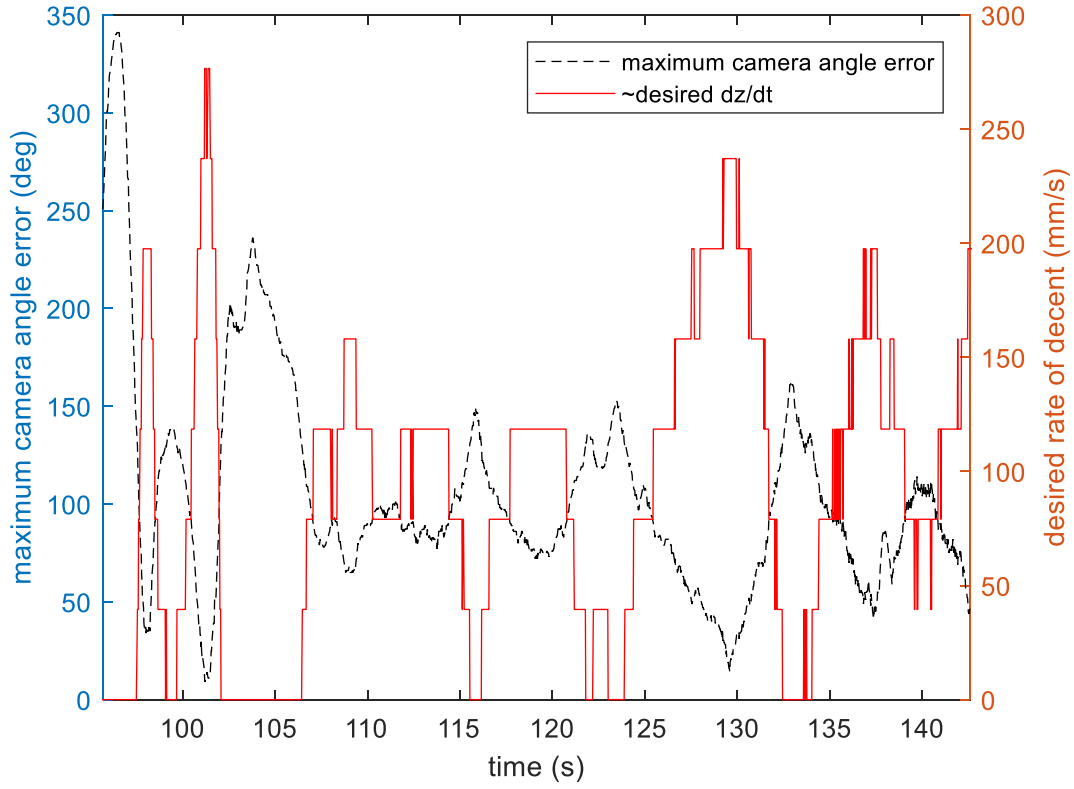

Figure 43: Max error and approximate desired change of altitude.

5.2 Additional Result Examples

5.2.1 Additional Test Results

The intention of this section is to provide some results from three outdoor flights. Figure 44 and Figure 45 are from the same test flight used in the description above. Unlike earlier, these plots here include information about the camera tilt and aircraft pitch. Figure 45 shows a similar trend as its counterpart in Figure 44 in that the camera angle compliments the commanded angle output in each of these.

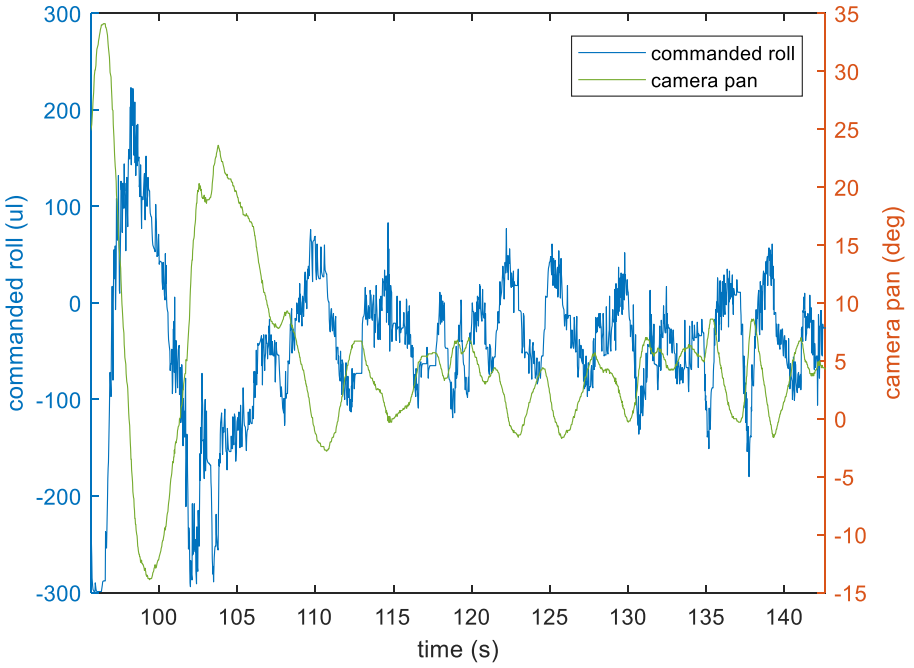

Figure 44: Camera pan and roll - Example flight 1.

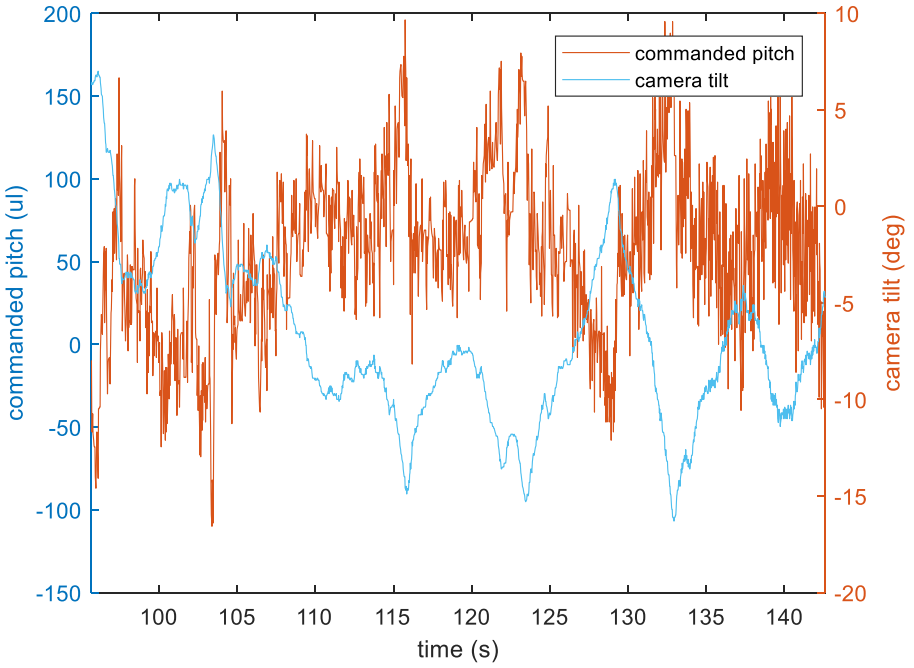

Figure 45: Camera tilt and aircraft pitch - Example flight 1.

Figure 46, Figure 47, and Figure 48 show the results from example flight 2. In this example, albeit different flight, the characteristics of flight are similar.

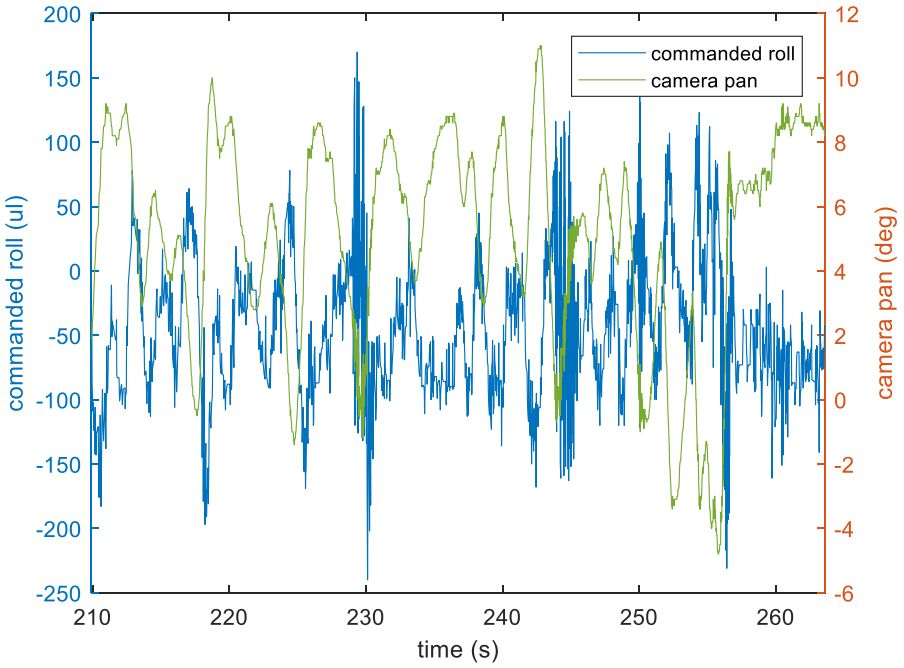

Figure 46: Camera pan and roll - Example flight 2.

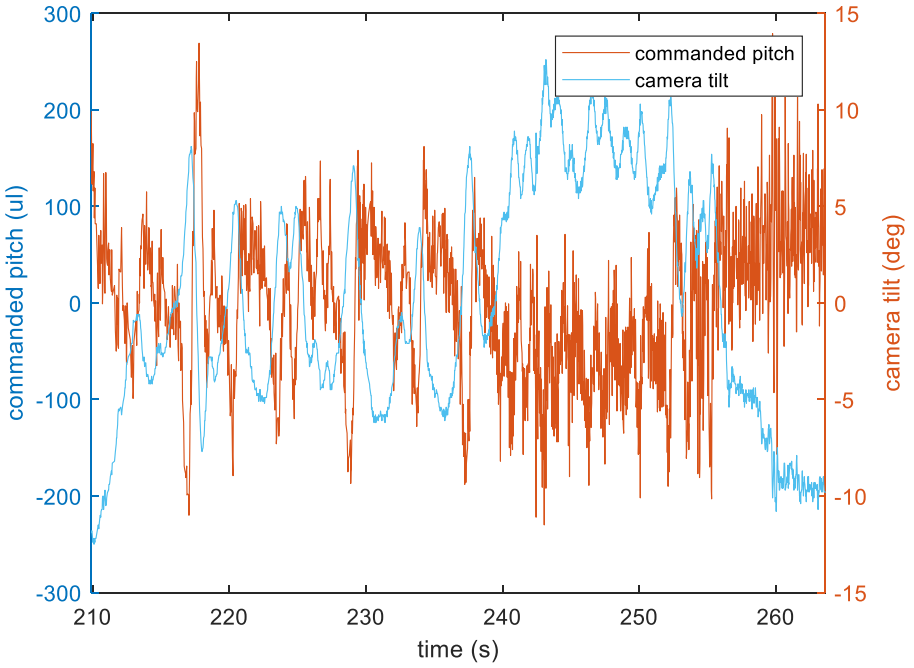

Figure 47: Camera tilt and aircraft pitch - Example flight 2.

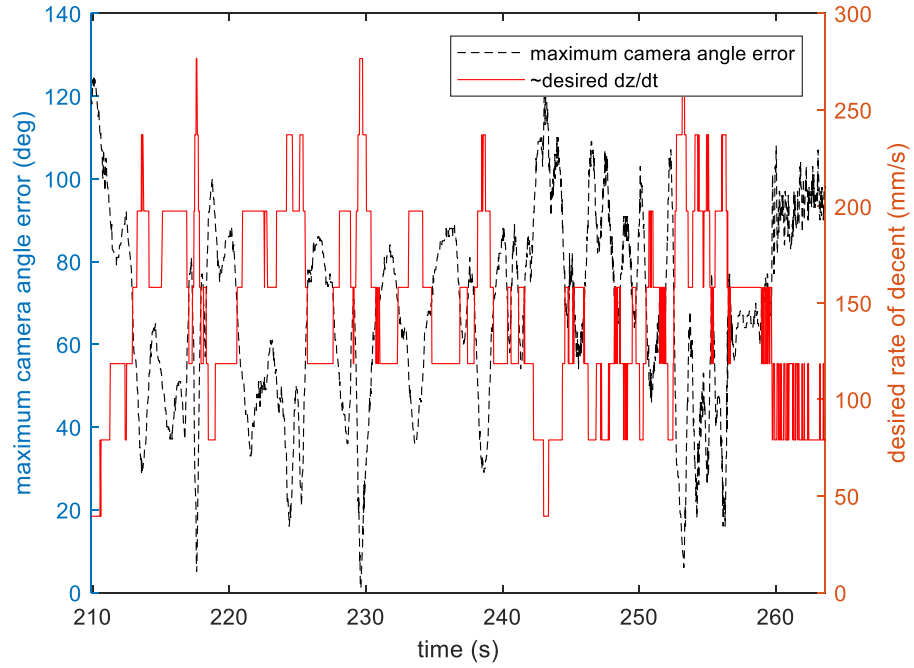

Figure 48: Maximum error and desired change in altitude - Example flight 2.

A final example is provided below in Figure 49, Figure 50, and Figure 51. Once again in Figure 49 and Figure 50 it is clear that the camera angles compliment the commanded orientation of the aircraft. Again seen in Figure 51 is that the aircraft commands faster descent as the camera angle errors are low.

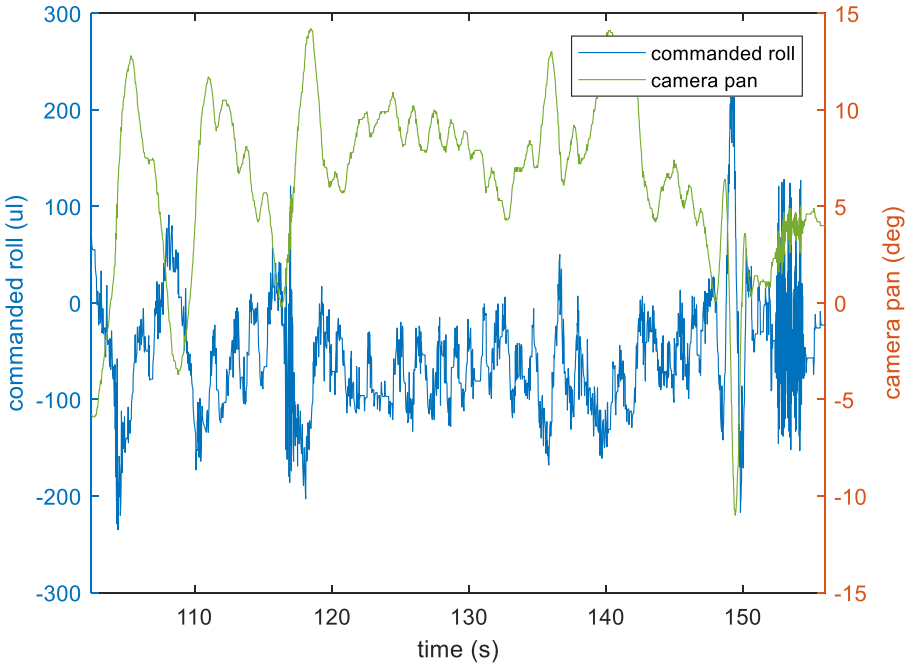

Figure 49: Camera pan and roll - Example flight 3.

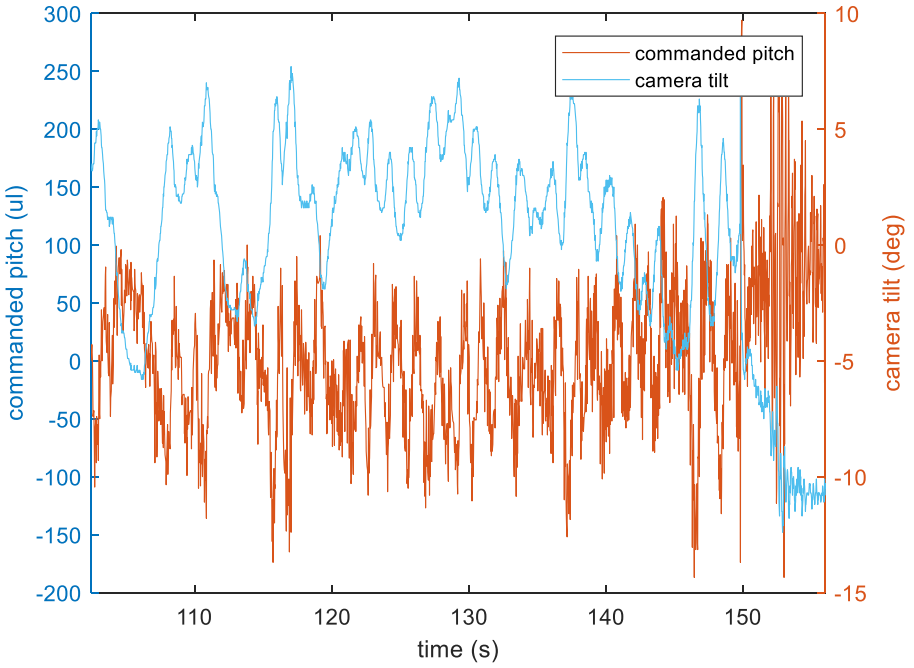

Figure 50: Camera tilt and aircraft pitch - Example flight 3.

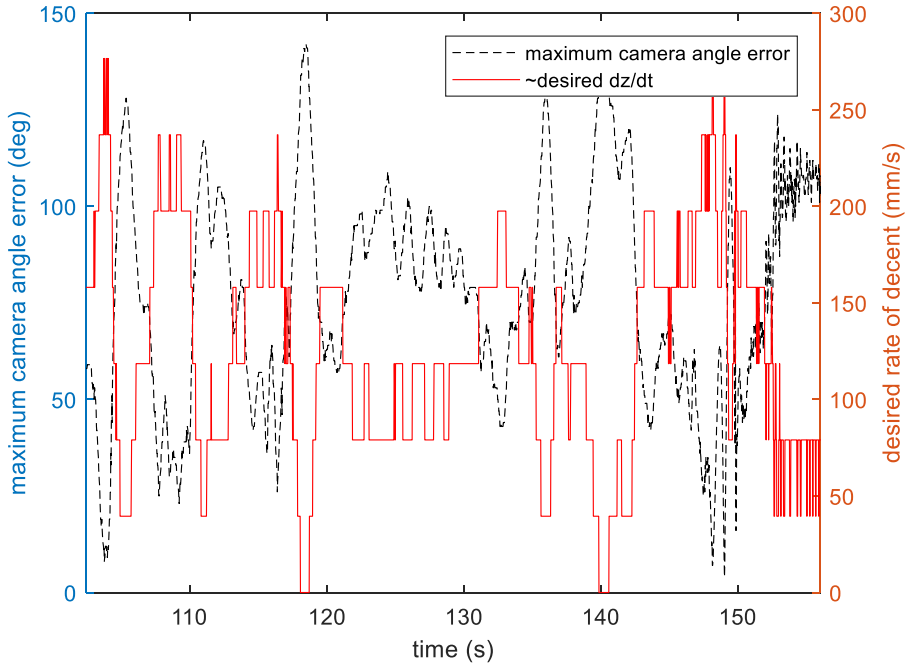

Figure 51: Maximum error and desired change in altitude - Example flight 3.

5.2.2 Photographs of Indoor and Outdoor Flight Tests

This section provides example images of aircraft flight. In Figure 52, the aircraft is mid-flight, early in the detection of the target location.

Figure 52: Indoor mid-air.

Figure 53 and Figure 54 show the aircraft approaching the dock location and positioning. It can be seen that the tip of the cone formed by the aircraft legs fits nicely into the ring.

Figure 53: Indoor approaching ring.

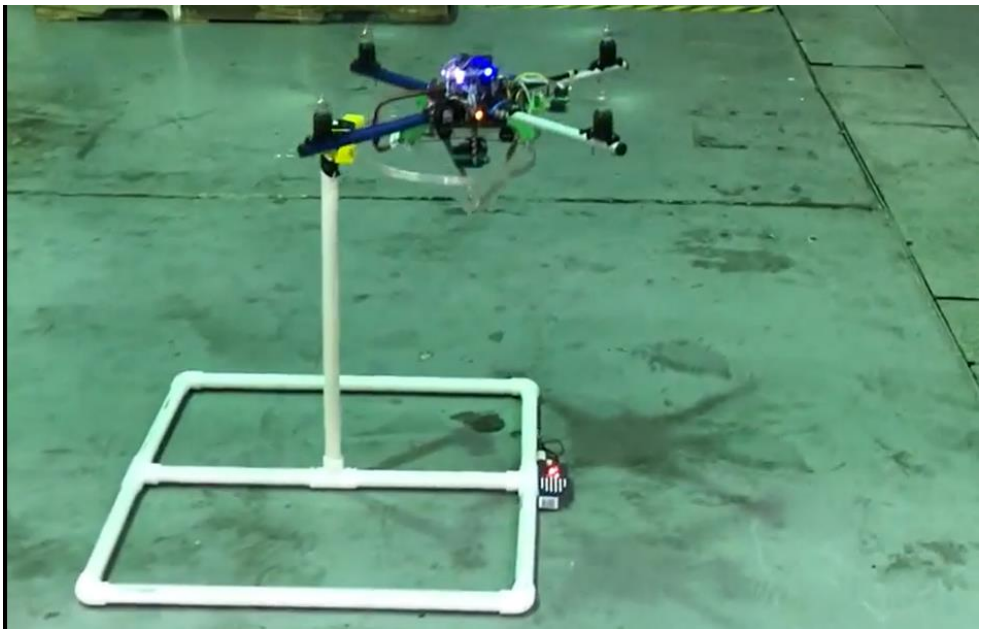

Figure 54: Indoor localizing.

Finally in Figure 55, the aircraft has positioned sufficiently and has actuated the legs of the aircraft. It is now attached to the ring.

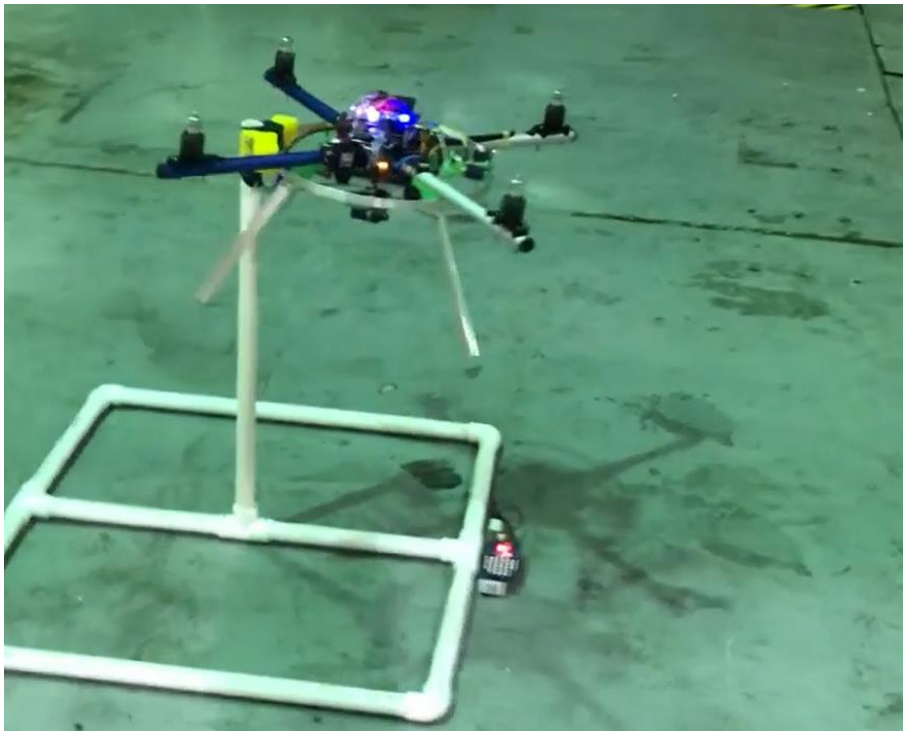

Figure 55: Indoor attachment.

Additional pictures of this process are shown below in Figure 56 through Figure 59. These images show that this system can also work in the non-ideal conditions of being outdoors. Again, these images show the aircraft hovering above the beacon, approaching, localizing and attaching to the dock location. Figure 56 shows the aircraft early in the autonomous landing procedure. Here the aircraft has detected the target and is positioning itself above it.

Figure 56: Outdoor midflight.

Figure 57 and Figure 58 show the aircraft approaching the ring and then positioning itself inside the ring.

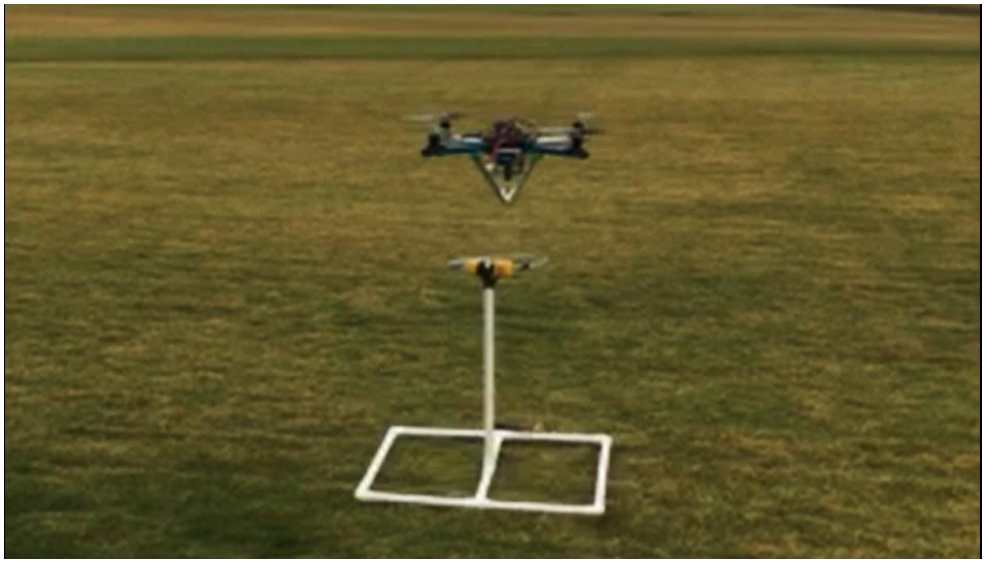

Figure 57: Outdoor approaching.

Figure 58: Outdoor localizing.

Once the aircraft is properly positioned, the legs are actuated, as shown in Figure 59, and the aircraft is attached to the ring.

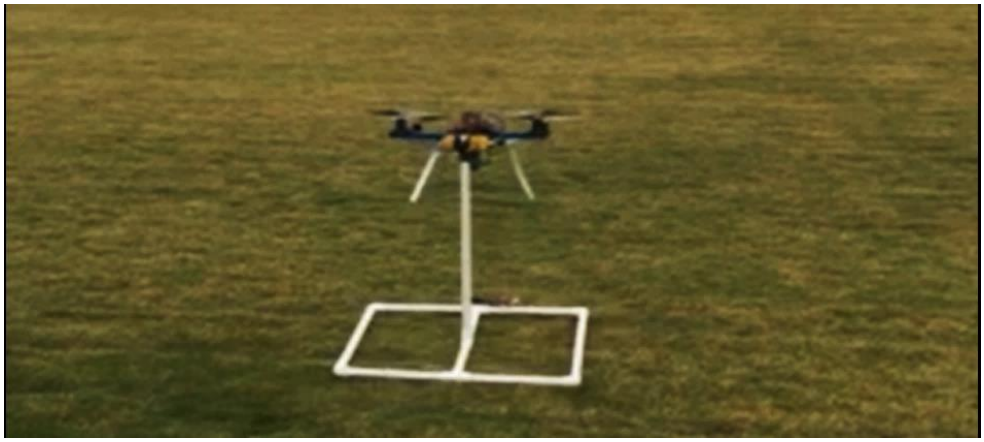

Figure 59: Outdoor attachment.

5.3 Future Work

This project was conceived with future applications in mind. The project will continue to complete the motivation of using this system for multi-aircraft cooperative lifting.

5.3.1 Changes to Initial Prototype

As this device is a prototype, there is inherent improvements that can be made. This section aims to provide several known (though small) issues and suggested improvements to future implementations of this system.

The gimbal subsystem is one such system that has some recommended improvements. As stated earlier, this system uses two digital micro servos to control the angle of the camera. These digital servos served their purpose reasonably well, but this system was assembled in-house. A professional grade gimbal would use brushless DC gimbal motors. Upgrading to a brushless gimbal motor system would mean faster, smoother motion of the camera which would improve the control of the device.

Furthermore, the gimbal as it is right now sometimes requires recalibration which is easily solved with better components.

Another change that would certainly be in the next version is to move the camera to the center of the aircraft body. This was not done in the current version as constant yaw angle was assumed. This meant that the camera could be off-center as long as the beacon has the same offset. This may be acceptable in future implementations, but to allow for maximum versatility of the device, it would be best to have the camera in the center of the aircraft and the beacon concentric with the ring. As stated earlier, the legs are designed to have a 45 deg angle relative to the boom when in Position 2. The ring design used a single piece of 3ft aluminium. This dictated the size of the ring which in turn dictated the separation of the legs from each other. As the legs were designed to have this 45 deg angle, the length of the legs was also constrained. With the inclusion of the actuating motor and battery, there was not enough room beneath the aircraft for the camera. This could be changed by either making the legs longer, using a different airframe, or modifications to this airframe to allow the battery to be placed elsewhere.

With respect to the legs of the aircraft, it is recommended in the future to determine leg sizes depending on application. This means that there should be stress modelling done to ensure the legs can support stresses in bad landing cases and withstand the forces acting on them due to a payload. For any payload to which the aircraft is attached, the length of the legs must be sized appropriately such that they will not deform while still maintaining clearance for transitioning between Positions 1 and 2. This is necessary as the angle of the legs in Position 1 is rather wide as to hold the ring, but this causes a greater bending moment on the legs when landing.

A final change that would be made is to the docking station. In this project, a rudimentary dock was made for proof of concept reasons. The future version should definitely allow the beacon to be mounted directly to the ring. Also, the ring should be a perfect circle as opposed to this one which has a plastic joint. This joint could interfere with the docking if the yaw angle is not constant relative to the ring as was done in this project.

5.4 Conclusion

The methods presented in this thesis, especially those of the attachment mechanism, may provide solutions for future use of UAVs in the commercial sector. A system such as this may be used for package identification, attachment, and subsequent transport. As autonomous UAVs become more common in daily life, this solution also satisfies the requirement for precision docking at home locations to store and charge aircraft.

REFERENCES

Al-Sharman, M. K. (2015). *Auto Takeoff and Precision Landing Using Integrated GPS/INS/Optical Flow Solution.* Sharjah, United Arab Emirates: American University of Sharjah.

Beardsley, P. A., Eriksson, M., Alonso-Mora, J., & Rehder, J. (2014). *United States of America Patent No. 2016/0039541 A1*.

Case for MarkOne Beacon. (2017, November 17). Retrieved from IR-Lock: https://irlock.com/collections/shop/products/case-for-markone-beacon?variant=13232506435

Dorie, J. (2017, June 28). *ELEV-8 Flight Controller Firmware*. Retrieved from Parallax: https://www.parallax.com/downloads/elev-8-flight-controller-firmware

ELEV-8 v3 Quadcopter Kit. (2017, November 17). Retrieved from Parallax: https://www.parallax.com/product/80300

Gentry, N. K., Hsieh, R., & Nguyen, L. K. (2014). *United States of America Patent No. 9,387,928 B1*.

Godzdanker, R., Valavanis, K. P., & Rutherford, M. J. (2010). *United States of America Patent No. 2014/0124621 A1*.

Jeffrey, J., Yanev, A., Biaz, S., & Murray, C. (2014). *UAV Quadcopter Landing on a Displaced Target (#CSSE14-05).* Auburn, AL: Auburn University.

Lovell, G., Hui, E. C.-K., & Umbreit, M. K. (2008). *United States of America Patent No. 2009/0294584 A1*.

Marshall, P. T. (2004). *United States of America Patent No. 7,398,946 B1*.

Prakash, A., & Ceribelli, M. (2014). *United States of America Patent No. 2016/0196756 A1*.

Precision Landing and Loiter with IR-LOCK. (2017, February 1). Retrieved from Ardupilot: http://ardupilot.org/copter/docs/precision-landing-with-irlock.html

Wang, M. (2014). *United States of America Patent No. 9,346,560 B2*.